7-10-2008

# Toward the Synthesis of Designed Metal-Organic Materials

Jacilynn A. Brant
*University of South Florida*

# Toward the Synthesis of Designed Metal-Organic Materials

by

Jacilynn A. Brant

A thesis submitted in partial fulfillment
of the requirements for the degree of
Master of Science
Department of Chemistry
College of Arts and Sciences
University of South Florida

Major Professor: Mohamed Eddaoudi, Ph.D.
Michael J. Zaworotko, Ph.D.
Julie P. Harmon, Ph.D.

Date of Approval:
July 10, 2008

Keywords: metal-organic materials, metal-organic frameworks, coordination polymers, molecular building blocks

## Table of Contents

## List of Figures

## List of Abbreviations

| Acronym | Full Name |
|---|---|
| 1,3-DAP | 1,3-Diaminopropane |
| 2,4-PDC | 2,4-Pyridinedicarboxylic acid |
| 2,5-PDC | 2,5-Pyridinedicarboxylic acid |
| 4-EIC | Ethyl 4-Imidazolecarboxylate |
| 4-ICA | 4-Imidazolecarboxylic acid |
| 4,5-IMDC | 4,5-Imidazoledicarboxylic acid |
| BU | Building Unit |
| DEF | N,N'-Diethylformamide |
| DMA | N,N'-Dimethylacetamide |
| DMF | N,.N'-Dimethylformamide |
| En | Ethylenediamine |
| EtOH | Ethanol |
| FT-IR | Fourier Transform Infrared |
| HMTA | Hexamethylenetetramine |
| MBB | Molecular Building Block |
| MOC | Metal-Organic Cube |
| MOF | Metal-Organic Framework |
| MOM | Metal-Organic Material |

| | |
|---|---|
| MOP | Metal-Organic Polyhedron |
| *n*MRs | *n* Member Rings |
| Pip | piperazine |
| SBB | Supermolecular Building Block |
| SCD | Single Crystal Diffraction |
| TBU | Tetrahedral Building Unit |
| TGA | Thermogravimetric Analysis |
| UV-Vis | Ultraviolet-visible |
| XRPD | X-Ray Powder Diffraction |
| ZMOF | Zeolite-like Metal-Organic Framework |
| ZIF | Zeolitic Imidazolate Framework |

**Toward the Synthesis of Designed Metal-Organic Materials**

**Jacilynn A. Brant**

## ABSTRACT

Metal-Organic Materials (MOMs) are an emerging class of crystalline solids that offer the potential for utilitarian design, as one of the greatest scientific challenges is to design functional materials with foreordained properties and eventually synthesize custom designed compounds for projected applications. Polytopic organic ligands with accessible heteroatom donor groups coordinate to single-metal ions and/or metal clusters to generate networks of various dimensionality. Advancements in synthesis of solid-state materials have greatly impacted many areas of research, including, but not limited to, communication, computing, chemical manufacturing, and transportation.

Design approaches based on building blocks provide a means to conquer the challenge of constructing premeditated solid-state materials. Single-metal ion-based molecular building blocks, $MN_x(CO_2)_{y+x}$, constructed from heterochelating ligands offer a new route to rigid and predictable MOMs. Specific metal bonds are considered responsible for directing the geometry or topology of metal-organic assemblies; these bond geometries constitute the building units, $MN_xO_y$. When these building units are connected through appropriate angles, nets or polyhedra can be targeted and synthesized, such as metal-organic cubes and Kagomé lattices. $MN_x(CO_2)_{y+x}$ MBBs can result in $MN_2O_2$ building units with square planar or see-saw geometries, depending on the mode of chelation. Using a 6-coordinate metal and a heterochelating

ligand with bridging functionality, TBUs can be targeted for the synthesis of valuable networks, such as Zeolite-like Metal-Organic Frameworks (ZMOFs).

Zeolitic nets, constructed from tetrahedral nodes connected through ~145° angles, are valuable targets in MOMs, as they inherently contain cavities and/or channel systems and lack interpenetration. Other design approaches have been explored for the design of ZMOFs from TBUs, such as the use of hexamethylenetetramine (HMTA) as an organic TBU. When this TBU coordinates to a 2-connected metal with appropriate angles, zeolite-like nets rare to metal-organic crystal chemistry can be accessed. Additionally, $MN_x(CO_2)_y$ MBBs have been used to construct metal-organic polyhedra (MOPs), used as supermolecular building blocks (SBBs), that can be peripherally functionalized and ultimately extended into three-dimensional ZMOFs.

Rational synthesis, mainly based on building block approaches, advances bridging the gap between design and construction of solid-state materials. However, some challenges still arise for the establishment of reaction conditions for the formation of intended MBBs and thus targeted frameworks.

## Chapter 1: Introduction to Metal-Organic Materials

Metal-Organic Materials (MOMs), a broad class that encompasses solid-state coordination polymers, metal-organic frameworks (MOFs), and metal-organic polyhedra (MOPs), generally consist of organic and metal monomers linked through metal-organic bonds.[1] Metal-organic interactions occur between metals and hetero-atoms, such as nitrogen, oxygen, sulfur and phosphorus. Polytopic ligands with accessible heteroatom donor groups coordinate to single-metal ions and/or metal clusters to generate networks of various dimensionalities. Commonly, MOMs are synthesized as crystalline materials; a crystal consists of atoms arranged in a pattern that repeats periodically in three dimensions.[2] The crystallinity of MOMs implies homogeneity throughout the solid phase, which expedites the processes of purification, characterization, property analysis and function determination. Crystalline materials aid understanding and development of design aspects for rational synthesis of solid-state materials. [3]

It has proven challenging to construct designed rigid, thermally stable MOMs that retain structural integrity and contain large cavities and/or channels void of interpenetration. However, frameworks have been successfully created by designing molecular building blocks (MBBs) that direct the formation of desired structures. Just as an architect must choose appropriate building material, (thatch, clay, or wood, etc.) for the project under construction, the MOM designer must deliberate appropriate metal and ligand combinations, and reaction conditions, to facilitate *in situ* formation and assembly of MBBs. It is essential that ligands contain appropriate chemical attributes, since much

of the resulting physical properties and the approaches to initially designing the material depend on it. Throughout the evolution of MOM research a wide range of organic linkers have been investigated for exploitation in design and synthesis, in conjunction with the inquiry of various metals.[4]

## 1.1 Overview of History

Early advancements in MOM development resulted mainly from serendipitous and fortuitous discoveries of appropriate reaction conditions for the crystallization of coordination polymers, and a crystalline MOM was structurally characterized as early as 1943.[5] Combinatorial processes, colloquially termed "shake and bake", yielded numerous interesting metal-organic nets and polyhedra, unveiling key knowledge associated with reactivity trends of hetero-atom donating ligands and metal ions and/or clusters for exploitation in the emergence of a new class of crystalline materials.

In the 1990's an exceptional amount of research on coordination polymers focused on the development of nitrogen-donating organic compounds,[6] such as pyridine- and cyano-derivatives, for use as monodentate, polytopic ligands. As early as 1959, there were reports of using organic ligands to form coordination polymers; specifically, a cyano-derivative was used as a linker between copper atoms in a coordination polymer with diamond-like topology.[8] A variety of MOMs, containing nitrogen-donating ligands have been synthesized and studied,[8-14] and ligands such as bipyridines,[15-17] dicyanobenzenes,[18-20] and cyanopyridines[21] commonly facilitate the formation of diamondoid networks.[22] An early example employs 4,4'-bipyridine (bpy) with an octahedral zinc metal ion to yield a square grid network. The 2-dimensional square grid layers pack ABAB and are catenated by perpendicular layers of square grids that also

pack ABAB. Through each of the four member rings (4MRs), a bpy ligand from a separate layer threads through to interweave the layers.

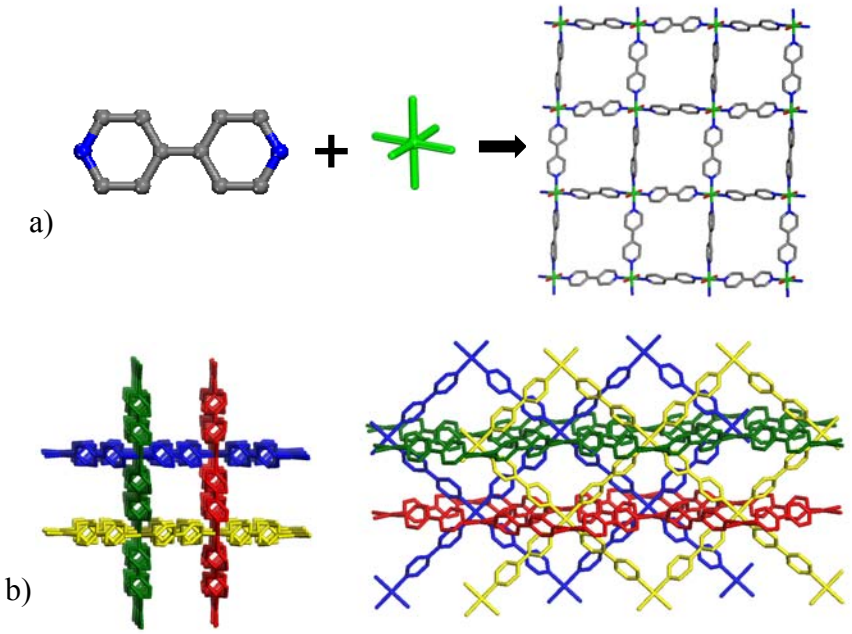


**Figure 1.1** (a) Reaction of 4,4'-bipyridine with zinc ions yields 2-D square grids (red=oxygen, blue=nitrogen, gray=carbon, green=zinc) that interpenetrate, and (b) individual layers are shown in red, green, blue, and yellow.[13]

Early examples of MOMs constructed from N-donor ligands were inclined to collapse and lack structural integrity upon removal or exchange of guest molecules, rendering them unsuitable for many applications.[23, 24]

After the initial eruption in investigations of N-donating ligands, carboxylates gained focus as linkers in design and synthesis of MOMs, with the anticipation of forming more rigid frameworks.[25-28] An interesting early example involves a coordination network, which contains 1,3,5-benzenetricarboxylic acid and cobalt, is comprised of 2-dimensional layers that are held together by mutual π-stacking of the pyridine guests with the benzene rings of BTC, which gives the framework physical properties that are closely related to that of 3-dimensional frameworks.[29] The compound,

able to selectively bind aromatic guests, is stable up to 350˚C, remains stable after removal of guests that can be selectively re-sorbed. Benzene, nitrobenzene, cyanobenzene, and chlorobenzene can all be adsorbed, while acetonitrile, nitromethane, and dichloroethane cannot be included within the framework. The selectivity of the framework is allegedly due to the π-stacking of the aromatic guests with the benzene portion of the BTC ligand.

Extensive research on incorporation of metal clusters, such as the copper-paddlewheel, has proven that adequate strength and inflexibility is provided through carboxylate coordination with metal ions for the design of MOMs. Crystallographic reports of the copper-paddlewheel occurred as early as 1823 by Brooke, research by Schabus, Groth, and Hull continued, and by 1953 J.N. van Niekerk and F.R.L. Schoening published the crystallographic data and structure of the mysterious cupric acetate molecule.[30] Dimetal, tetracarboxylate paddlewheel clusters can be employed as square building blocks, containing other 6-coordinate metals, such as zinc, cadmium, and nickel, to construct MOMs.[31-32] Other examples utilize the axial positions of the paddlewheel for coordination by bridging ligands to result in networks with nodes of higher connectivities. Figure 1.2. illustrates the use of the paddlewheel cluster as a 6-connected node, as 4,4'-bipyridine bridges axial positions.

Several other carboxylate based building units have been used in the design and synthesis of MOMs, such as the octahedral "basic zinc acetate" cluster and the trigonal prismatic oxo-centered trimer.[1] Many MOMs have utilized carboxylate-metal clusters as nodes and some possess unique applications.[31-32, 34-35]

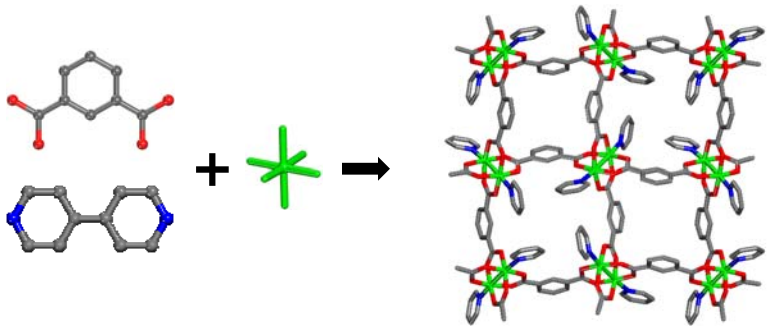

**Figure 1.2.** The use of the paddlewheel cluster as a 6-connected node is illustrated, as 4,4'-bipyridine bridges axial positions. [31]

Numerous carboxylate containing coordination compounds have been produced and encompass high porosity and a conglomeration of novel functionalities, including, but not limited to magnetism and gas storage. Networks encompassing paddlewheel and other chelated carboxylate building blocks have proven to be thermally stable upon removal of guests.[25,27]

Exuberant studies have been based on applications of porous MOFs comprised of modifiable organic carboxylate-based linkers and metal cluster nodes, which is evident from the unveiling of a class of isoreticular porous materials,[25, 36-37] in which every compound has the same framework topology of $CaB_6$. Sixteen different organic ligands were used as linkers to create the sixteen porous MOFs that constitute this class of compounds. Every compound in the series has a higher percent free volume than the most open zeolite, faujasite, and the family of compounds is thermally stable up to temperatures between 300˚ and 400˚C [25]. The isoreticular family consists of frameworks composed of octahedral Zn-O-C clusters, $[OZn_4]^{6+}$, and various ditopic carboxylate linkers. The utilization of ditopic ligands of differing lengths yields structures containing various pore sizes with varying gas storage capabilities.

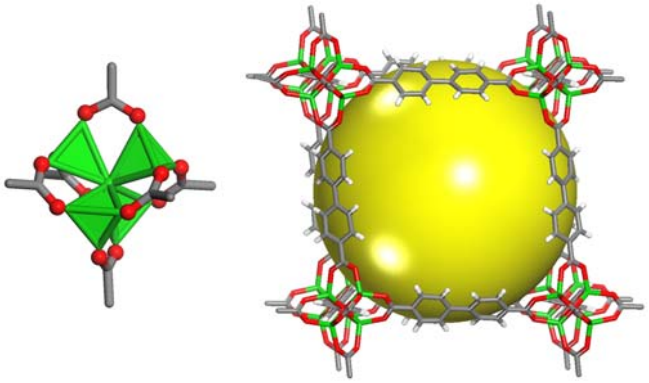

**Figure 1.3.** The basic zinc acetate cluster (left), composed of four tetrahedral metal ions coordinated by six carboxylates to form a 6-coordinate node, that is used to construct various IRMOFs with analogous topology to $CaB_6$ (right).[36]

This work embraces many possibilities and exhibits numerous opportunities that MOF research can offer. This study provides evidence that a specific network can be extended by consistently accessing a targeted building block. It has been proven that utilization of different organic ligands can result in different properties and thus unique functionalities.

A plethora of diverse linkers have been utilized in the construction of various ionic and neutral MOFs. Anionic MOMs are generated in the presence of cations, such as amines, to create charge balance,[38-40] and several cationic MOFs have been constructed as well.[41-43] In addition to the numerous ionic frameworks, there are also examples of neutral MOFs,[44-45] and the synthesis thereof lacks the necessity for charge compensating ions. Neutral, anionic, and cationic ligands can be employed in the directed synthesis of materials with predisposed ionic strengths, dependant mainly on the charge of building components and metal to ligand ratios.

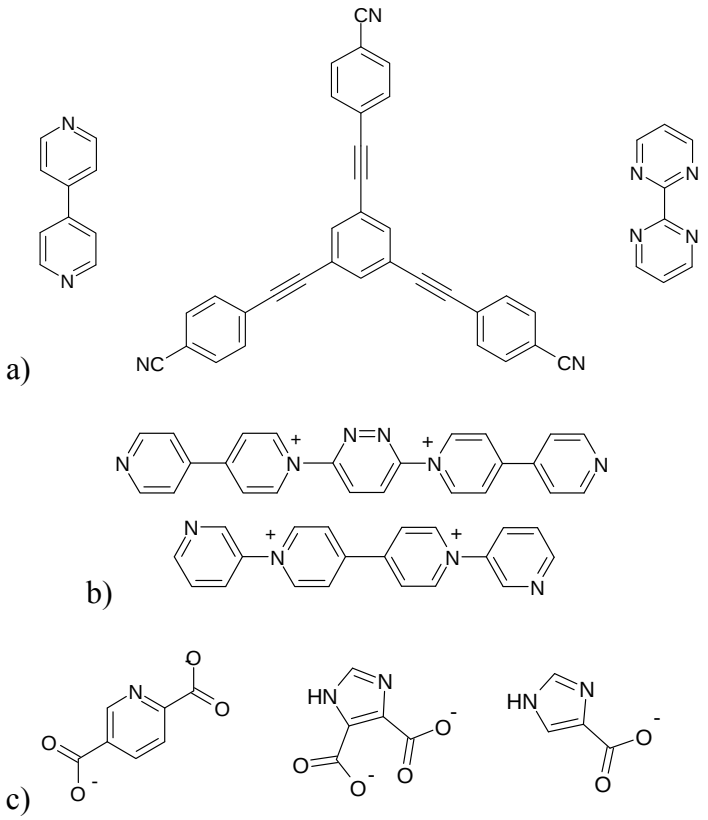


**Figure 1.4.** a) Neutral, b) cationic, and c) anionic ligands can be used in the synthesis of MOFs with varying ionic strengths.

Anionic MOMs are of extreme interest due to the potential use as metal-organic platforms that can be chemically tweaked *via* post-synthetic and/or ship-in-bottle ion-exchange. In addition, the geometrics of organic and inorganic cations can be exploited to direct the formation of intended structures.

## 1.2 Fundamentals

MOMs can be simplified and structurally explained in terms of nodes and spacers, as shown by Robson in the late 1980's and early 1990's, [9, 46-47] in which a node is generally any site in the network with more than two connectivities and a linker exhibits two connections. Metal-organic structures are classified as zero dimensional (discrete), one dimensional (chains), two dimensional (layers), and three

dimensional. Discrete MOMs, not supporting or requiring the notion of continuity, generally exist as geometrically distinct polygons and polyhedra, such as a metal-organic squares and cubes. Metal-organic chains can be comprised of linear, zig-zag and ladder-like connectivities. Two- and three-dimensional networks are classified in terms of topology, an extension of geometry.

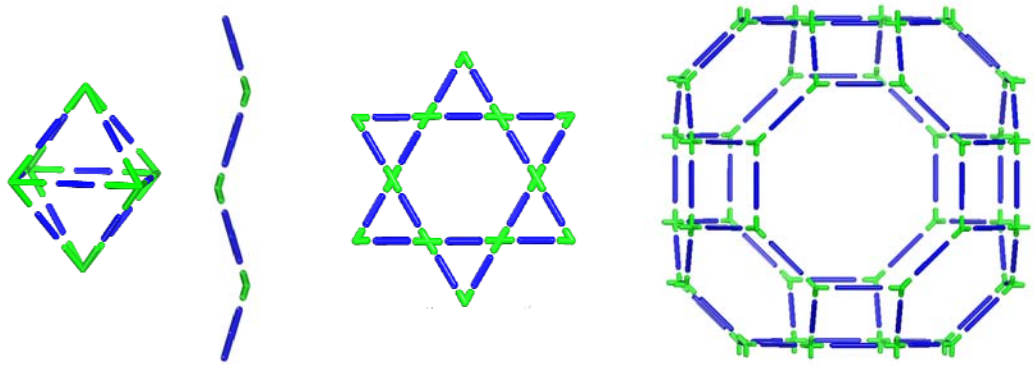

**Figure 1.5.** 0-, 1-, 2-, 3-D (left to right) metal-organic materials depicted with nodes (green) and spacers (blue).

Topological descriptors, such as coordination sequences and vertex symbols are used to identify and distinguish nets. The notion of coordination sequence (CS) was formally introduced by Brunner & Laves in 1971[48] in order to investigate the topological identity of frameworks and of atomic positions within a framework. Each node, or vertex, in a framework has a CS, and, in an abstract sense, the CS explains the growth of a network. For example, (Figure 1.6.) the coordination sequence for the tetrahedral node in *lta* is 4, 9, 17, 28, 42, 60, 81, 105, 132, 162, which implies the first node (blue) is connected to 4 nodes (red), while those nodes are connected to 9 nodes (yellow), and the 9 nodes are connected to 17 nodes (green), etc. The coordination sequence $\{N_x\}$ is a sequence $N_1$, $N_2$, $N_3$… that shows the total number of atoms in the 1$^{st}$, 2$^{nd}$, 3$^{rd}$ …. coordination spheres.[49]

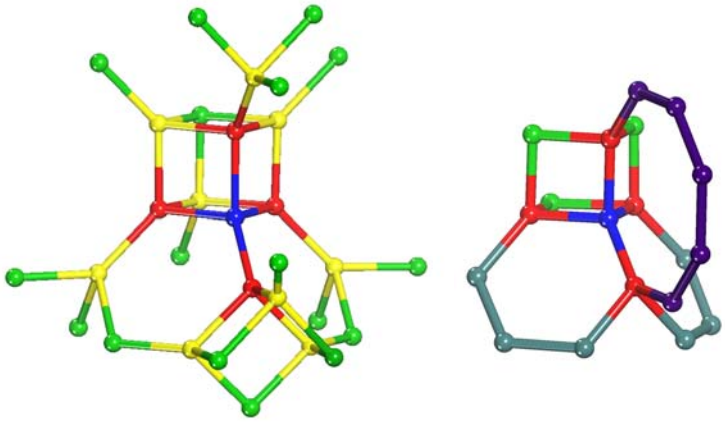

**Figure 1.6.** The coordination sequence (4, 9, 17, 28, 42, 60, 81, 105, 132, 162) and vertex symbol (4.6.4.6.4.8) of the *lta* net are displayed.

Vertex symbols indicate the size of rings that occupy a node. The symbols for opposite pairs of angles are grouped together and rings of the same size at a vertex are indicated by a subscript or superscript, depending on the notation used. Additionally, the Schläfli symbol, named for the nineteenth century mathematician Ludwig Schläfli, lists the numbers and sizes of circuits starting from any non-equivalent atom in the net. In the Schläfli symbol $A^a.B^b.C^c$, the length (number of nodes in a ring) of each shortest cycle is signified by A, B, C… and number of types of rings by a,b,c... The extended Schläfli symbol lists all shortest circuits for each angle for any non-equivalent atom. Other notations are also used to list such descriptors, including Wells and O'Keeffe. For example, the vertex symbol of *lta* is 4.6.4.6.4.8 begins with 4.6 as smallest circuit is a 4MR which is opposite to a 6MR.[50]

In crystal chemistry, the formation of regular nets is common, and sometimes unavoidable. The regularity of a net is categorized in terms of transitivity, *pqrs*, which specifies the number of kinds of vertices (*p*), edges (*q*), essential rings (*r*), and tiles (*s*). For example, the transitivity of the *dia* net is 1111, therefore it is a regular net and thus

highly favorable for formation in crystal chemistry. Essentially, transitivities, although composed of four digits, can be viewed as a single number; more regular nets have lower numerical transitivities and are generally more easily accessed by the metal-organic material designer. The *lta* net has the transitivity 1343. The three edges can be viewed as (1) the edge between squares and hexagons, (2) the edge between squares and octagons, and (3) the edge between hexagons and octagons. There are four types of faces, which are determined by congruency and symmetry. The net has three types of tiles, $[4^6]$, $[4^6.6^8]$, and $[4^{12}.6^8.8^6]$.

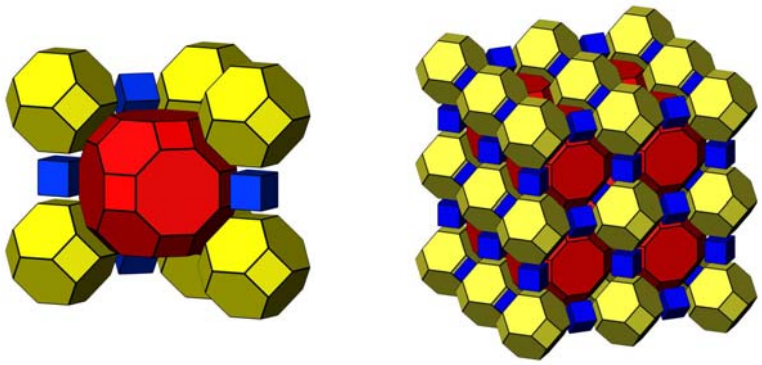

**Figure 1.7.** The *lta* net contains three types of tiles $[4^6]$ (blue), $[4^6.6^8]$ (yellow), and $[4^{12}.6^8.8^6]$ (red).

The *lta* net and others with similar attributes are targeted networks in MOMs for applications relying on porosity, as the tiles can be translated into metal-organic cages. The tiles pack in a manner to expose intersecting channels. Such porous structures can be classified according to spatial dimensions of the pores or cavities, which include zero-dimensional (dots), one-dimensional (channels), two-dimensional (layers), and three-dimensional pore systems (intersecting channels).[4] 3-D pore systems are extremely useful due to the induced mobility of guests or solvent molecules. Various layered MOFs, containing 2-D pore systems, have been reported, however most of them are unable to

host several guests. Guest molecules residing in 1-D pore systems are free to move in one direction, while guests present in 0-D pore systems are isolated from other cavities and are unable to pass to other cavities. The possible applications of a specific porous material are generally dependant on the type of pore system that is embedded within the framework. Research involving porous materials has been developing for many years. Essentially, a permanently porous framework remains robust, without reversible or irreversible collapse, during guest loss, which results in a stable framework that contains a vacuum in the channels of the framework.[35]

## 1.3 Challenges

The most significant challenge associated with MOMs is to combine knowledge of chemical reactivity, crystallization techniques, and basic nets with aspects of utilitarian function to design and synthesize materials for specific applications. Although some frameworks containing nitrogen-donating ligands are robust, thus far, the employment of carboxylate-containing ligands and metal-clusters have been more widely employed in creating irreversibly porous open frameworks.[26, 65] N-donating ligands have been proven to act as effective linkers in MOFs, however, the typical flexibility of the M-N bond impedes topological design[39] and monodentate N-based ligands do not commonly result in permanently porous nets.[66,67]

## 1.4 Advancements/Developments

Carboxylate-based ligands continue to be used in the synthesis of MOMs with some of the largest cavities exhibited in solid-state materials. For example, an exceptional material, namely MIL-101, is constructed from chromium and terephthalate with cages about 34Å in diameter and an unprecedented free volume of about 702,000

Å$^3$.[52] A mesoporous MOF, made with triazine-1,3,5-tribenzoic acid and terbium, has been reported with two types of cages, one with 39 Å and the other 47 Å in diameter.[53] Advances in design and rational synthesis of targeted materials, with large cavities/channels void of interpenetration, continue to benefit applications,[54] such as catalysis,[55-57] gas storage,[58-59] and sensing[60].

Recently, it has been demonstrated that imidazole-based linkers that exhibit monodentate coordination can successfully be used for the construction of Zeolitic Imidazolate Frameworks (ZIFs). ZIFs are constructed by the coordination of imidazolate and imidazolate-type linkers to tetrahedral single metal ions, such as Co and Zn. These examples prove that extensive exploration of reaction conditions can allow access to zeolite-*like* topologies, and thus avoidances of diamond-like networks. ZIFs have surface areas up to 1,970m$^2$/g, thermal stability and exceptional chemical stabilities. Additionally, these porous frameworks are suitable for gas storage and can selectively capture $CO_2$ from $CO/CO_2$ mixtures.[51]

# Chapter 2: Introduction to Rational Synthesis of Metal-Organic Materials

## 2.1 Overview

Serendipitous discoveries have been very fruitful and will continue to yield valuable solid-state materials and insights to design. Although much progress in research pertaining to solid-state materials has been made,[3,35] the same basic synthetic approaches have been utilized for the majority of the twentieth century.[61] Recently, synthesis of solid-state compounds progressively resembles rational approaches used in other fields of chemistry, such as organic chemistry, due to the use of building blocks. Unlike organic chemistry, which involves the union of building blocks in a stepwise fashion, or by one functional group at a time, synthesis of solid-state materials is feasibly viewed as concerted processes. The fact that all bond-making and bond-breaking is considered simultaneous explicates the great challenges associated with positioning chemically active groups in a manner to facilitate intended interactions. Perhaps, one day synthesis of solid-state materials will entirely entail pre-designed systematic approaches that will allow synthetic researchers to design made-to-order materials. Currently, it is often possible to predict likely structures that result from certain building blocks,[28] but the challenge remains to actually synthesize designed materials, while avoiding non-target nets that may have more favorable formation. Approaches based on the use of molecular building blocks (MBBs) offer great potential.

## 2.2 Fundamentals

As mentioned earlier, networks with lower numerical transitivities are easier targets in crystal chemistry. Transitivity classifications aid the MOM designer to envision and anticipate the formation of specific nets from regular vertex figures. While some of these nets are exciting for some applications, other, less regular nets with analogous coordination figures are often targeted. By understanding the types of nets that are likely to form, one can target avoiding certain structures in order to obtain those with higher transitivities.

| Z | Coordination Figure | Name | Transitivity |
|---|---|---|---|
| 3 | triangle | ***srs*** | 1111 |
| 4 | square | ***nbo*** | 1111 |
| 4 | tetrahedron | ***dia*** | 1111 |
| 6 | octahedron | ***pcu*** | 1111 |
| 8 | cube | ***bcu*** | 1111 |
| 12 | cuboctahedron | ***fcu*** | 1112 |
| 4 | rectangle | ***lvt*** | 1121 |
| 4 | tetrahedron | ***sod*** | 1121 |
| 4 | tetrahedon | ***lcs*** | 1121 |
| 4 | tetrahedron | ***lcv*** | 1121 |
| 4 | tetrahedron | ***qtz*** | 1121 |
| 6 | hexagon | ***hxg*** | 1121 |
| 6 | metaprism | ***lcy*** | 1121 |
| 6 | octahedron | ***crs*** | 1122 |
| 6 | octahedron | ***bcs*** | 1122 |
| 6 | trigonal prism | ***acs*** | 1122 |
| 8 | tetragonal prism | ***reo*** | 1122 |
| 8 | bisdisphenoid | ***thp*** | 1122 |
| 4 | rectangle | ***rhr*** | 1132 |
| 4 | tetrahdedron | ***ana*** | 1132 |

**Figure 2.1.** Regular, quasi-regular, and semi-regular nets, classified by transitivity, are prime targets for the synthesis of pre-designed networks.[61-62]

Regular nets are defined to have symmetry that requires a regular polygon or polyhedron coordination figure, or viewed in terms of natural tiling, in which the

| Z | Coordination Figure | Name | Trans. |
|---|---|---|---|
| 4,8 | tetrahedron, cube | ***flu*** | 2111 |
| 3,6 | triangle, octahedron | ***pyr*** | 2112 |
| 4,12 | square, cuboctahedron | ***ftw*** | 2112 |
| 4,8 | quadrangle, cube | ***sqc*** | 2121 |
| 3,4 | triangle, square | ***pto*** | 2122 |
| 3,4 | triangle, tetrahedron | ***bor*** | 2122 |
| 3,4 | triangle, tetrahedron | ***ctn*** | 2122 |
| 3,6 | triangle, octahedron | ***spn*** | 2122 |
| 4,6 | square, octahedron | ***soc*** | 2122 |
| 4,6 | square, hexagon | ***she*** | 2122 |
| 4,6 | tetrahedron, octahedron | ***toc*** | 2122 |
| 4,6 | tetrahedron, octahedron | ***gar*** | 2122 |
| 4.6 | tetrahedron, octahedron | ***ibd*** | 2122 |
| 4,12 | tetrahedron, ocoshedron | ***ith*** | 2122 |
| 6,6 | octahedron, trigonal prism | ***nia*** | 2122 |
| 3,4 | triangle, rectangle | ***tbo*** | 2123 |
| 3,8 | triangle, tetragonal prism | ***the*** | 2123 |
| 3,12 | triangle, truncated tetrahedron | ***ttt*** | 2123 |
| 4,6 | tetrahedron, octahedron | ***iac*** | 2123 |
| 4,24 | octahedron, truncated octahedron | ***twf*** | 2123 |
| 6,8 | octahedron, cube | ***ocu*** | 2123 |
| 6,12 | hexagon, truncated tetrahedron | ***mgc*** | 2123 |
| 3,24 | triangle, rhombicuboctahedron | ***rht*** | 2123 |
| 4,4 | quadrangle, quadrangle | ***ssc*** | 2131 |
| 4,4 | rectangle, tetrahedron | ***pts*** | 2132 |
| 4,4 | rectangle, tetrahedron | ***pth*** | 2132 |
| 4,6 | rectangle, trigonal prism | ***stp*** | 2133 |
| 4,8 | rectangle, tetragonal prism | ***scu*** | 2133 |
| 4,12 | rectangle, hexagonal prism | ***shp*** | 2133 |
| 6,12 | trigonal prism, hexagonal prism | ***alb*** | 2134 |
| 4,4 | quadrangle, quadrangle | ***ssa*** | 2143 |
| 4,4 | quadrangle, quadrangle | ***ssb*** | 2143 |
| 4,8 | quadrangle, cube | ***csq*** | 2155 |

**Figure 2.2.** Edge transitive, binodal nets represent a class of lucrative nets to target.[63-64]

transitivity is equal to 1111.[63] Such nets, as *srs* and *dia,* have been referred to as default nets for 3-D nets, for triangular and tetrahedral nodes, respectively. These types of nets

crystallize frequently, especially from building blocks that lack rigidity, and are commonly unavoidable. A quasi-regular net, *fcu,* is vertex-, edge-, and face-transitive, 1112 and semi-regular nets have 11*rs* transitivities.[62] For example, semi-regular net *sod* has 1121 transitivity and is described as vertex, edge, and tile transitive. Vertex transitive nets are referred to as uninodal and edge transitive as isotoxal and represent easily accessible networks. In addition to regular, quasi-regular, and semi-regular nets, binodal edge transitive nets are feasible targets for rationally constructed materials.

Recent MOM design includes expansion of known networks selected as targets, which are often prevalent in nature. An approach, coined "top-down design, bottom up synthesis,"[39] entails the following process. First, the target network should be intellectively anatomized, or deconstructed into essential building blocks of specific geometry, directionality, and connectivity that are required for the construction of the network. Organic ligands and metals, which can be exploited to construct appropriate MBBs, are deliberated to essentially construct the targeted network.[34] Geometrical information of the intended coordination figures are recreated with a linker or combination of linkers, single-metal ions, and/or metal clusters. Building blocks should be rigid in order for the geometric information to be retained during network assembly. Linkers that remain rigid allow more control of the binding angle between the extensions of the polytopic linkers. When designing porous materials, nonflexible building blocks are beneficial for the creation of rigid frameworks that will remain permanently porous upon evacuation of guests. When single metal nodes are utilized, ligands should be able to lock the metal into position, causing rigidity of the entire framework.

As an example of expansion, in which the distance between the vertices of the target framework is increased, the zeolite net *rho* is targeted. It can be realized that *rho* consists of α-cages, or truncated cuboctahedra ($[4^{12}.6^{8}.8^{6}]$). The cages connect through a double 8 member ring (d8MR), resulting in a body centered cubic arrangement, to yield a 3-dimensional channel system of 8MRs. The cages are composed of twelve 4MRs, eight 6MRs and six 8MRs. The framework can be further dissected to reveal that each of these rings, and ultimately the α-cage, is essentially built from 4-coordinate tetrahedral nodes.

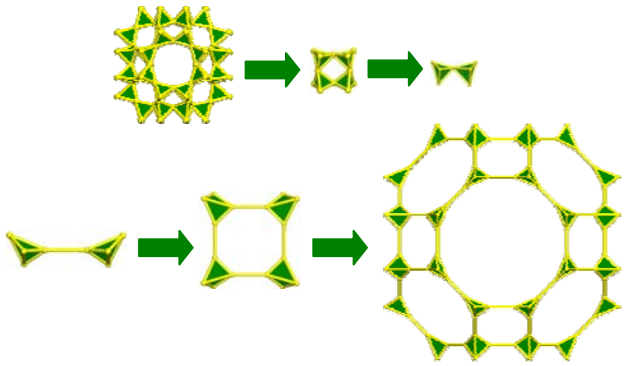

**Figure 2.3.** The *rho* net can be intellectively dismantled to an essential tetrahedral building units linked through an approximate 145° angle and consequently rebuilt and expanded using metal-organic molecular building blocks (MBBs).[65]

Assembly of tetrahedral coordination figures is likely to result in regular nets, such as *dia, sod, lcs, lcv,* etc., therefore, more information must be invested in the MBBs to avoid such regular nets. The 48 tetrahedral nodes are connected through an average angle of 145°. Next, one must determine which metals and ligands can be exploited to construct a MBB that is rigid, tetrahedral and facilitates 145° angle connections. This particular case demonstrates that a metal with 8-coordination sites can be combined with a ditopic heterochelating ligand to form 4-coordinate tetrahedral building units (TBUs). 4,5-imidazoledicarboxlate (4,5-IMDC) has the capability to act as a ditopic N-, O-heterochelating ligand and the metal-nitrogen bonds can be used to direct the topology,

while carboxylate oxygen atoms can lock the metal nodes into position. 4,5-IMDC contains nitrogen atoms oriented to facilitate connection of metal nodes though ~145° angles.

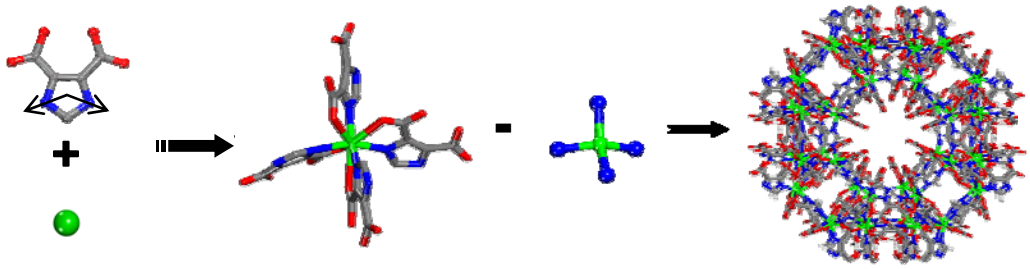

**Figure 2.4.** 4,5-IMDC and $In^{3+}$ are used to make a TBU for the assembly of anionic *rho*-ZMOF.

Under experimentally ascertained solvothermal conditions, the indium-based MBBs assemble *in situ* and a zeolite-*like* MOF (ZMOF) with *rho* topology, namely *rho*-ZMOF, is constructed. Expansion is accomplished, and the cavities can accommodate a sphere with approximate diameter of 18.2 Å. The unit cell is approximately 8 times larger than the aluminosilicate zeolite *rho*. [65]

## 2.3 Challenges

A key to targeting materials is considering the plethora of possible outcomes and narrowing the list by introducing constrictive components. Challenges remain in the selection of suitable MBBs for coordination figures of targeted nets, and ultimately metal and ligand combinations. As the qualifications for metals and ligands are realized for construction of MBBs for targeted materials, reaction conditions must be established for the formation and assembly of the MBBs. Under relatively mild conditions, the polytopic linkers and the appropriate metal nodes must be linked, retaining rigidity and geometric information throughout the synthesis, to form MOMs having the desired topology. Both

the linkers and nodes must have attributes that accommodate the intended coordination figures, and commonly more intelligence must be incorporated to avoid simple nets. It is important that the MBB is rigid and geometrically inductive, as structure ductility may defy the intention of avoiding certain high-symmetry, simple nets. As the MBB of interest is realized, reaction conditions for assembly must be discovered. As many interesting nets commonly result from the same coordination figure, a MBB should be reproducible in the presence of slight variations, such as ligand length for expansion, structure directing agents (SDAs) for versatility, and functionalization for utility. Determination of adequate reaction conditions is the remaining challenge to catenate design and synthesis of the target materials.

## 2.4 Advancements/Developments

A single-metal ion-based MBB approach employs ligands that contain a nitrogen atom in the α-position relative to a carboxylate group, which facilitate the formation of 5-membered rings of chelation, with metal ions capable of high coordination numbers to form rigid and robust frameworks.[68] Generally, chelates of higher denticity will result in building blocks with more predictable orientations than monodentate ligands. Potentially, metal-nitrogen bonds will direct the topology of the resultant network, while oxygen atoms can be used to complete the coordination sphere of single metal vertices, locking the metals into position through chelation. This approach combines the directionality induced by N-donating ligands and the rigidity of frameworks built from metal-clusters. Incorporating rigid building blocks into MOM design will enhance structure prediction. Utilizing heterochelating ligands with geometrically stringent

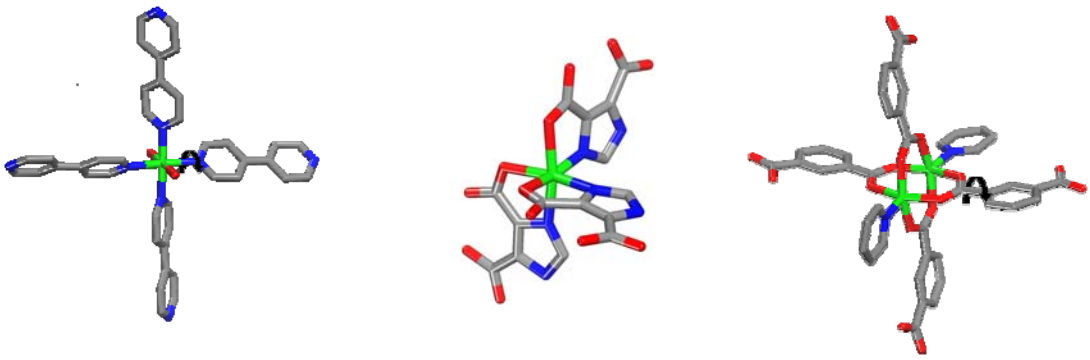

**Figure 2.5.** Rigid $MN_3(CO_2)_3$ MBB, from a heterochelating ligand, (center) has a rigid geometry, while the N-based building block (left) and paddle-wheel building block (right) show the potential for bond rotations.

bridging capabilities allows access to targeted, and sometime rare and unprecedented, framework topologies in metal-organic crystal chemistry. In certain cases, general conditions for the formation of specific MBBs have been established. Sometimes, these established conditions can be used for the synthesis of isoreticular networks of varied metals and/or ligands. Additionally, some results imply that certain conditions are successful for specific ligand families and certain types of metals. For established methods, such as the formation of paddlewheel building blocks from metal ions and carboxylate-based ligands, simple conditions containing appropriate metal-to-ligand ratios and N,N'-dimethylformamide solvent systems can be applied to various nodes and spacers. Trends can be analyzed from results of combinatorial chemistry and employed in the directed synthesis of materials.

## Chapter 3: Single-Metal Ion-based Molecular Building Block Approaches for the Advancement of Metal-Organic Material Design

### 3.1 $MN_x(CO_2)_y$ Molecular Building Blocks Constructed from Nitrogen- and Carboxylate-Based Heterochelating Ligands

The directionality of the nitrogen-based ligands and the rigidity of carboxylate-based MOFs are combined by incorporating heterochelating capabilities into judiciously designed ligands. The strategy to design and synthesize metal-organic assemblies consists of the formation of rigid and directional single-metal-ion based MBBs, namely

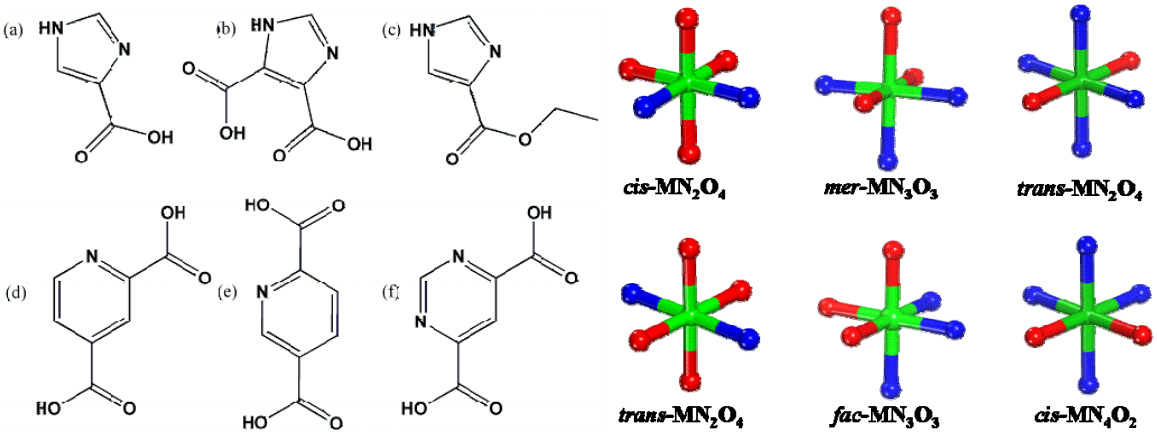


**Figure 3.1.** (Left) Heterochelating ligands with bridging functionality: (a) 4-imidazolecarboxylic acid, (b) 4,5-imidazoledicarboxylic acid, (c) 4-imidazolethanoate, (d) 2,4-pyridinedicarboxylic acid, (e) 2,5-pyridinedicarboxylic acid, and (f) 4,6-pyrimidinedicarboxylic acid. (Right) Isomers of $MN_xO_y$ single metal ions.

$MN_x(CO_2)_{x+y}$ that contain *x* N-, O- chelating moieties, and *y* bridging carboxylates. Such ligands, which possess both the chelating and bridging functionality, are shown in Figure 3.1.

Herein, 4-connected nodes, derived from MBBs based on 6-coordinate single-metal ions, $MN_xO_y$, ($x + y = 6$), will be considered for the construction of robust metal-organic assemblies. Specifically, MBBs are targeted from *cis*- and *trans*- isomers of $MN_2O_4$ and $MN_4O_2$ and *fac*- and *mer*-isomers of $MN_3O_3$ using directional ligands, such as 2,5-PDC, 2,4-PDC, 4,5-IMDC, Et 4-IMCand 4-IMC.

### 3.1.1 $MN_4O_2$ Single Metal Ions in Molecular Building Blocks

$MN_4O_2$ single-metal ions can be formed by the coordination of various types of heterochelating ligands, including those with two nitrogen donor atoms and one carboxylate group, such as 4-imidazolecarboxylate. $MN_4(CO_2)_2$ MBBs yield building units (BUs), which direct the topology, with seesaw or square planar geometries. In contrast with the geometries of $MN_2O_2$ BUs, derived from $MN_2(CO_2)_4$ MBBs, which rely on chelation and coordination modes, the geometry of the resultant $MN_4$ BUs from $MN_4(CO_2)_2$ is dependant only on the mode of coordination. Obviously, since the nitrogen atoms are responsible for directing network topologies, the configuration of coordination directs framework formation.

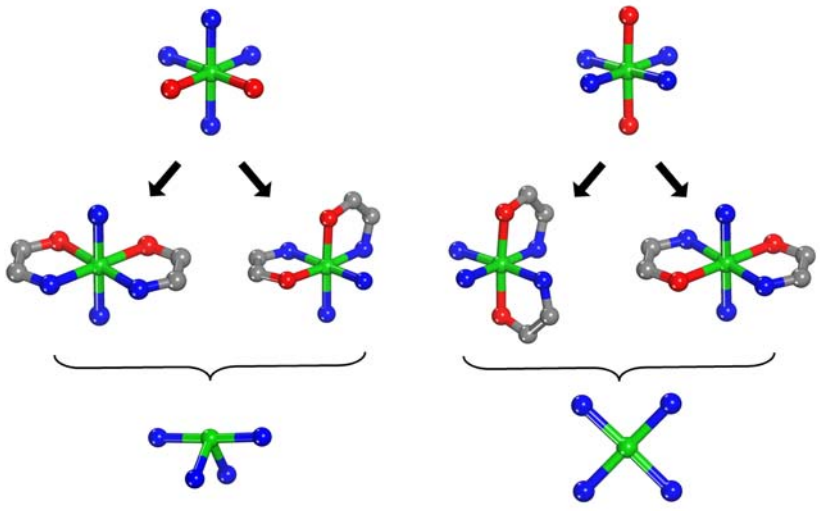

**Figure 3.2.** $MN_4O_2$ single metal ions can be used to access seesaw- and square planar-like building units.

### 3.1.2. $MN_2O_4$ Building Units derived from $MN_2(CO_2)_4$ Molecular Building Blocks

Two types of configurational isomers, *cis*- and *trans*-, are accessible in the octahedral hetero-coordinated single metal ion $MN_2O_4$, resulting in various types of MBBs in which topological directors have square planar-like or see-saw-like geometries. The *trans*-$MN_2(CO_2)_4$ MBB can yield a square-planar-like building unit (BU), which results from *trans*-chelation[66] and a see-saw-like BU is a product of *cis*-chelation. Three possible types of MBBs can be constructed from *cis*-type coordination, depending on the sites of chelation, from which different SBUs can be derived. Configurational *cis*-isomers bear two types of see-saw-like SBUs as well as a square planar-like SBU (Fig. 3.3).

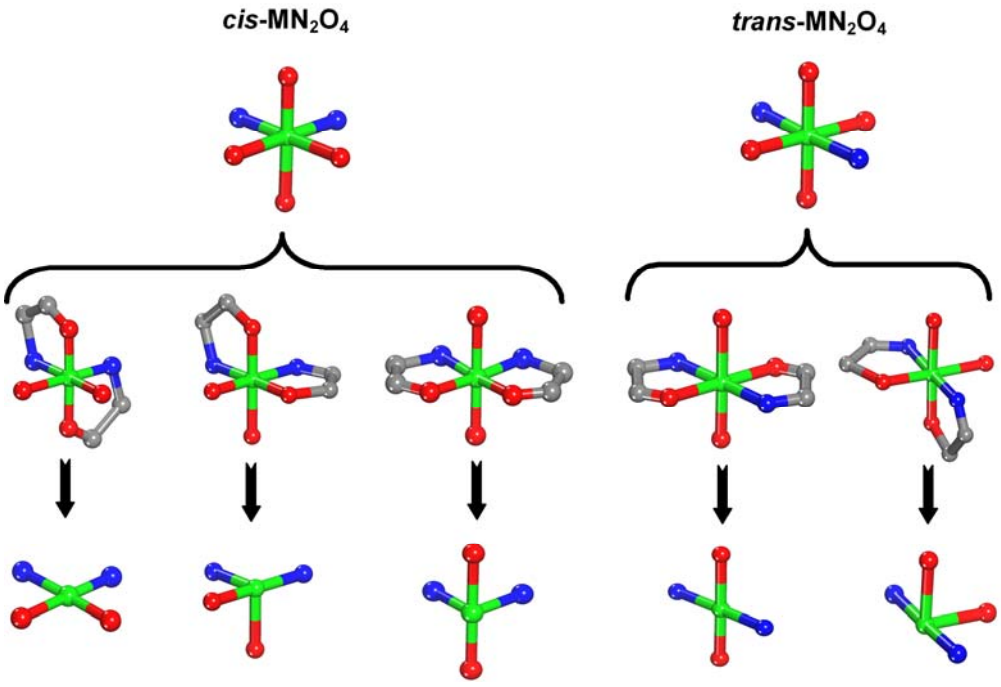


**Figure 3.3.** Heterochelating ligands can coordinate to single-metal ions to result in $MN_2(CO_2)_4$ molecular building blocks that act as 4-connected square-planar- and see-saw-*like* building units.

We have previously reported[67] the congregation of single-metal-ion-based MBBs, with the general formula $InN_2(CO_2)_4$, resulting in the assembly of two supramolecular

isomers, a Kagomé lattice and a $M_6L_{12}$ octahedron from the heterochelating ligand 2,5-PDC. The metal-organic Kagomé lattice consists of 4-connected MBBs, exhibiting *cis*-chelation, that act as square-planar BUs. The discrete $M_6L_{12}$ octahedron is constructed from an $InN_2(CO_2)_4$ MBB that constitutes a see-saw-like BU. In both examples, a multifunctional heterochelating and bridging ligand, 2,5-pyridinedicarboxylate, connects the nodes through ~120° angles to configure the rationally expected networks. The rigid, geometry inducing ligand, 2,5-pyridinedicarboxylate, links the single-metal ions to generate a discrete MOF of the $M_6L_{12}$ octahedron. Yet another MOF, involving the multifunctional 2,5-pyridinedicarboxylate ligand, includes a configurational *cis*-isomer of the single-metal-ion and thus the $MN_x(CO_2)_y$ MBB, namely $FeN_2(CO_2)_4$. The $FeN_2(CO_2)_4$ represents the third type of MBB, in which *cis*-chelation affords a see-saw-like SBU. In this type of see-saw, two different types of atoms are present in the lever and the fulcrum, as opposed to the see-saw-like SBUs found in the isoreticular octahedron structures that have one type of atom in the lever (oxygen) and the other type (nitrogen) in the fulcrum. The see-saw-like MBBs assemble, through the multifunctional linkers, to yield a MOF related to the cubic diamond net. This work demonstrates that by accessing different MBBs, and thus different BUs, with a consistent ligand (2,5-PDC), various networks can be formed.[68]

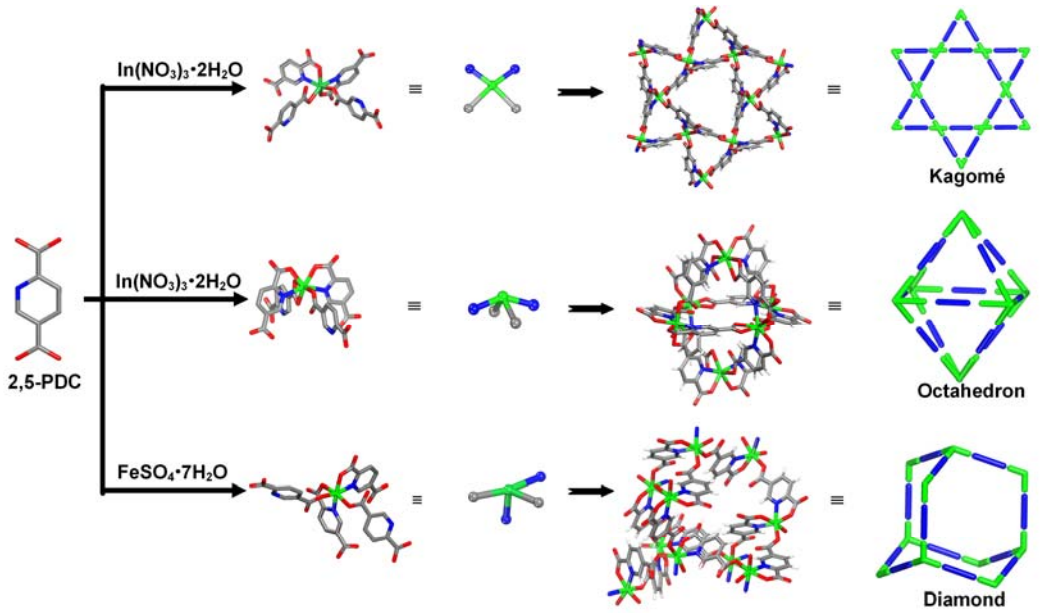


**Figure 3.4.** $MN_2(CO_2)_4$ MBBs are used to construct a metal organic Kagomé lattice, an octahedron, and diamond-like net.[68]

### 3.1.3 $MN_3O_3$ Building Units derived from $MN_3(CO_2)_3$ Molecular Building Blocks

The $MN_3O_3$ octahedral single-metal ion can exist as two possible geometric isomers, the *fac*-isomer and the *mer*-isomer (Figure 3.5). As the nitrogen atoms are considered to direct the topology of resultant structures, two types of BUs are accessible from this type of coordination, namely *mer*-$MN_3$ from *mer*-$MN_3(CO_2)_3$ and *fac*-$MN_3$ from *fac*-$MN_3(CO_2)_3$ Examples of the *mer*-$MN_3(CO_2)_3$ MBB exist,[69-71] but to our knowledge, these types of MBBs involving 5-member rings of chelation are rarely reported as part of extended coordination polymers. However, extended structures involving analogous non-chelating *mer*-$MN_3O_3$ building blocks have been synthesized.[72] Previously, we have reported the occurrence of *fac*-$NiN_3(CO_2)_3$, in which the facial metal-nitrogen bonds topologically direct the formation of a cube (Figure 3.6).[73] It is

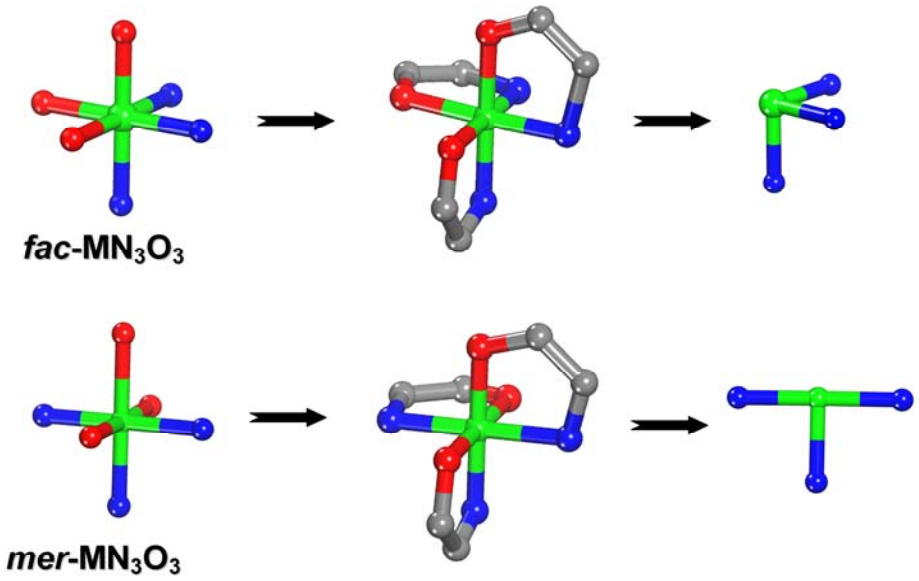


**Figure 3.5.** $MN_3(CO_2)_3$ molecular building blocks can be viewed an *fac*- (top) or *mer*-$MN_3O_3$ (bottom) building units.

apparent that the majority of the crystal structures containing tris-chelated octahedral nickel, $NiN_3(CO_2)_3$, deposited on the Cambridge Structural Database (CSD) have facial geometry. The metal-nitrogen bonds of the MBB geometrically constitute the corner of a cube and $NiN_3(CO_2)_3$ has been employed in edge-directed assembly of an anionic metal-organic cube (MOC-1), which has Ni-Ni-Ni angles within the range of 88.28(1) to 91.85(1)˚.

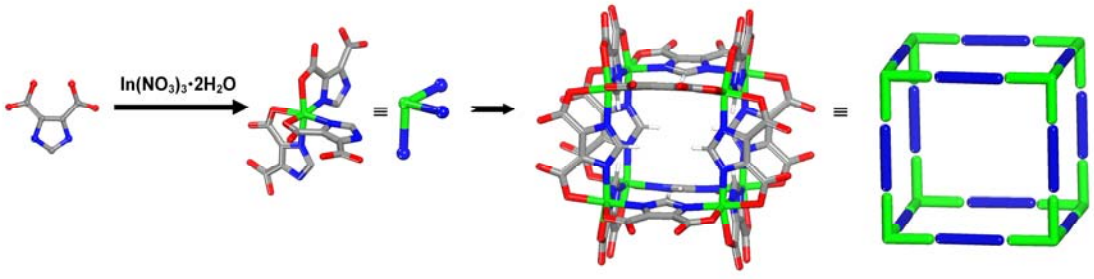


**Figure 3.6.** A metal-organic cube is constructed from a *fac*-$NiN_3(CO_2)_3$ MBB.[73]

## 3.2 Experimental

All chemicals were used as received from Fisher Scientific, Sigma-Aldrich, and TCI America chemical companies. Fourier transform infrared (FT-IR) spectra were measured using an Avatar 320 FT-IR system. Absorptions are described as follows: very strong (vs), strong (s), medium (m), weak (w), and broad (br). X-ray powder diffraction (XRPD) data were recorded on a Rigaku RU15 diffractometer at 30kV, 15mA for $Cu_{K\alpha}$ ($\lambda$ = 1.5418 Å), with a scan speed of 1°/min and a step size of 0.05° in 2$\theta$. Calculated XRPD patterns were produced using PowderCell 2.4 software. Single-crystal X-ray diffraction (SCD) data were collected on a Bruker SMART-APEX CCD diffractometer using $Mo_{K\alpha}$ radiation ($\lambda$ = 0.71073 Å) operated at 2000 W power (50 kV, 40 mA). The frames were integrated with SAINT software package[74] with a narrow frame algorithm. The structure was solved using direct methods and refined by full-matrix least-squares on $|F|^2$. All crystallographic calculations were conducted with the SHELXTL 5.1 program package,[75] and performed by Dr. Victor Kravtsov, Dr. Lukasz Wojtas, Dr. Derek Beauchamp, Dr. Rosa Walsh or Gregory J. McManus in the Department of Chemistry at the University of South Florida. Crystallographic tables are included for each compound in Appendix I

Olex[76] and Topos[77] software was used to determine topological representations of the obtained MOMs, and the resulting terms compared to those in the literature and the RCSR database.[50] Total solvent-accessible volumes were determined using PLATON[78] software by summing voxels more than 1.2 Å away from the framework. Tiling was evaluated using 3dt software.[79]

**Synthesis of {[Cd(4-ICA)$_2$]}$_n$, ME086**. $Cd(NO_3)_2 \cdot 4H_2O$ (9mg, 0.0435mmol) and 1*H*-imidazole-4-carboxylic acid (4-ICA) (7.3mg, 0.0653mmol) were added to a solution of DMF (1mL), water (0.5mL), imidazole (1.46M in DMF, 0.1mL) and nitric acid (2.85M in DMF, 0.225mL) in a 20mL scintillation vial. The reaction was heated at a rate of 1.5°C/min to 85°C for 12h, cooled to r.t. at 1°C/min, yielding colorless faceted polyhedral crystals. Experimental XRPD: 14.0, 18.1, 19, 23.5, 26.2. Calculated XPRD: 13.92, 18.18, 19.08, 23.1, 26.4, 28.06, 29.52, 31.8, 32.4, 35.0, 36.0, 37.06, 39.6

**Synthesis of {[Cd(4,5-IMDC)(en)]}$_n$, ME089** Cadmium (II) acetate dihydrate(0.0435mmol, 11.6mg) was added to 4,5-IMDC (0.087mmol, 13.6mg) in the presence of DMF (1mL), and nitric acid (350μL of 2.96 M in DMF). The reaction was heated to 65°C at 1.5°C/min. The reaction remained at 65°C for 12h and was then cooled to room temperature at a rate of 1°C/min. Experimental XRPD: 9.7, 11.5, 15.5, 18.0, 19.4, 25.1; Calculated XRPD: 7.86, 8.82, 9.66, 10.63, 11.38, 11.96, 15.4, 15.7, 17.8, 19.4, 20.2, 20.93, 22.4, 25.3, 26.6, 27.35, 30.8, 34.1.

**Synthesis of [In$_6$(2,5-PDC)$_{12}$], ME694.** $In(OAc)_3 \cdot H_2O$ (0.0435mmol) and 2,5-pyridinedicarboxylic acid (0.087mmol) were added to a solution of DMA (1mL) and 0.1mL 0.058 M piperazine/DMF in a 20mL scintillation vial. The reaction was heated at a rate of 1.5°C/min to 85°C for 12h, cooled to r.t. at 1°C/min Colorless block-like crystals resulted IR: 3156.7 (br), 1667 (m), 1566 (s), 1482.2 (w), 1395(s), 1350.9 (s), 1266 (w), 1104 (w), 1018.8 (m), 942.4 (w), 834 (s), 756.9 (s), 694.7 (w), 648.6 (w). Experimental

XRPD: 5.17, 6.16, 6.41, 7.029, 8.14, 8.89, 9.75, 10.62, 11.61, 11.98. Calculated XRPD: 5.1, 6.02, 6.45, 6.8, 7.0, 7.45, 7.95, 8.85, 9.75, 9.9, 10.61, 11.04, 11.2, 11.64, 12.02, 13.1, 13.3, 13.66, 13.96, 14.25, 15.77, 15.9, 16.33, 16.9, 17.5, 18.1, 20.3, 21.83.

.

**Synthesis of $\{[Cd(4\text{-}ICA)_2]\}_n$, ME207**. $Cd(NO_3)_2 \cdot 4H_2O$ (9mg, 0.0435mmol) and 1*H*-imidazole-4-carboxylic acid (4-ICA) (7.3mg, 0.0653mmol) were added to a solution of DMF (1mL), water (0.5mL), imidazole (1.46M in DMF, 0.1mL) and nitric acid (2.85M in DMF, 0.225mL) in a 20mL scintillation vial. The reaction was heated at a rate of 1.5°C/min to 85°C for 12h, cooled to r.t. at 1°C/min, yielding colorless faceted polyhedral crystals. Experimental XRPD: 13.2, 14.304, 19.71. Calculated XPRD: 7.16, 9.27, 10.19, 12.07, 13.08, 14.35, 14.96, 16.62, 16.6, 20.45, 21.25, 21.97, 22.56, 23.13, 23.69, 24.44, 25.22, 25.66, 30.19, 30.75, 36.35

**Synthesis of $\{[Cd(4\text{-}IMC)(H_2O)]\}_n$, ME096.** $Cd(NO_3)_2 \cdot 4H_2O$ (7.5mg, 0.0217mmol) and 4-ICA (4.9mg, 0.0435mmol) were added to a solution of DMF (0.5mL), water (0.125mL), 4,4'-trimethylenedipiperidine (0.95M in DMF, 0.05mL) and nitric acid (2.85M in DMF, 0.1mL) in a 20mL scintillation vial. The reaction was heated at a rate of 1.5°C/min to 85°C for 12h, cooled to r.t. at 1°C. Colorless block-like crystals resulted Experimental XRPD: 7.7, 15.4, 21.9, 23.6, 26.6; Calculated XRPD: 7.7, 15.5, 22, 23.5, 26.7

**Synthesis of $[Cd_8(4,5\text{-}IMDC)_{12}]$, ME299**. $Cd(OAc)_2 \cdot 2H_2O$ (232mg, 0.87mmol) and 2,5-PDC) (340mg, 2.18mmol) were added to a solution of N,N'-diethylformamide (DEF)

(20mL), ethanol (EtOH) (10mL) and HMTA (1.42M in $H_2O$, 2mL) in a 20mL scintillation vial. The reaction was heated at a rate of 1.5°C/min to 85°C for 12h, cooled to r.t. at 1°C/min, heated to 105°C and cooled to r.t. yielding colorless octahedral-like crystals. Experimental XRPD: 12.1, 15.9, 17.5, 19.9, 20.6, 26.2, 28.1, 29.8, 32.9, 35.2; Calculated XRPD: 10.2, 12.1, 12.7, 14.6, 15.9, 16.3, 17.9, 19, 20.7, 21.6, 22, 23.4, 24, 24.4, 25.5, 26.2, 27.5, 28.3, 33, 36.3, 37

**Synthesis of $[Cd(4,5\text{-IMDC})(en)]_n$, ME511**. $Cd(OAc)_2 \cdot 2H_2O$ (11.6mg, 0.0435mmol) and ethyl 4,5-IMDC (13.6mg, 0.087mmol) were added to a solution of DMA (0.75mL), En (2.96M in DMF, 0.325mL) and EtOH (0.5mL) in a 20mL scintillation vial. The reaction was heated at a rate of 1.5°C/min to 85°C for 12h, cooled to r.t. at 1°C/min, yielding colorless octahedron-like crystals. Experimental XRPD: 13.5, 14.0, 16.3, 18.9, 20.0, 26.0. Calculated XRPD: 11.95, 13.3, 14.1, 15.6, 16.14, 18.7, 19.4, 19.96, 23.3, 25.8, 28.3, 30.2, 27.05.

**Synthesis of $[Cd(4\text{-EIC})_2]_n$, ME184**. $Cd(NO_3)_2 \cdot 4H_2O$ (13mg, 0.0435mmol) and ethyl 1*H*-imidazole-4-carboxylate (4-EIC) (12mg, 0.087mmol) were added to a solution of DMF (2mL), and EtOH (1mL) in a 20mL scintillation vial. The reaction was heated at a rate of 1.5°C/min to 85°C for 12h, cooled to r.t. at 1°C/min, yielding colorless faceted polyhedral-like crystals. IR: 1727(s), 1685 (w), 1604 (w), 1505 (s), 1392 (m), 1266 (w), 1193(s), 11.76 (s), 1138 (s), 1024 (m), 966 (s), 896 (s), 852 (s), 677 (s). Experimental XRPD: 10.663, 15.184, 21.436, 28.588; Calculated XRPD: 10.67, 13.14, 15.05, 15.18, 16.9, 18.55, 21.44, 22.79, 23.92, 25.15, 25.3, 27.39, 28.54, 30.37, 30.95, 31.5, 37.6.

**Synthesis of Formula, $[Cd_3(4,5\text{-IMDC})_4 \cdot DMF]_n$, JB9545.** $Cd(OAc)_2 \cdot 2H_2O$ (11.6mg, 0.0435mmol) and 4,5-IMDC (13.6mg, 0.087mmol) were added to a solution of DMA (0.75 mL), and EtOH (0.5mL) and en (0.325mL 2.96M in DMF) in a 20mL scintillation vial. The reaction was heated at a rate of 1.5°C/min to 85°C for 12h, cooled to r.t. at 1°C/min, heated to 105°C for 23h, cooled to r.t., heated to 105°C for 23h and cooled to r.t. yielding colorless hexagonal plate-like crystals. XRPD: 6.26, 7.18, 7.83, 8.51, 9.89, 10.43, 13.11, 15.14, 18.56; Calculated XRPD: 6.27, 7.19, 8.51, 9.7, 10.25, 10.4, 11.25, 13.2, 18.88, 24.2

**Synthesis of $[Cd_6(4,5\text{-IMDC})_{10}]_n$, ME688.** $Cd(OAc)_2 \cdot 2H_2O$ (11.6mg, 0.0435mmol) and 4,5-IMDC (13.6mg, 0.087mmol) were added to a solution of DMA (0.75 mL), DEF (1.25mL) and 1,3-DAP (0.1mL). The reaction was heated at a rate of 1.5°C/min to 85°C for 12h, cooled to r.t. at 1°C/min, yielded colorless faceted polyhedral crystals. Experimental XRPD: 3.7, 4.7, 6.3, 8.4, 9.1, 11.7, 14.7; Calculated XRPD: 3.87, 4.67, 6.2, 8.35, 9.04, 11.15, 11.65, 14.63, 14.92, 18.13

## 3.3 Results & Discussion

### 3.3.1 MOMs resulting from $MN_4O_2$ Single-metal ion-based Building Blocks

A reaction between a 1:2 ratio of cadmium nitrate and 4,5-IMDC in the presence of ethylenediamine yielded a metal-organic zig-zag chain, $\{[Cd(4,5\text{-IMDC})(en)]\}_n$ (ME089) The ditopic ligand chelates to the cadmium in a bidentate fashion. However, two of the binding sites on the metal are occupied by ethylenediamine, which acts as a

terminal ligand. Due to the unintended coordination of ethylenediamine, 2-connected building units, $CdN_2$, result from the assembly of $CdN_4(CO_2)_2$ MBBs.

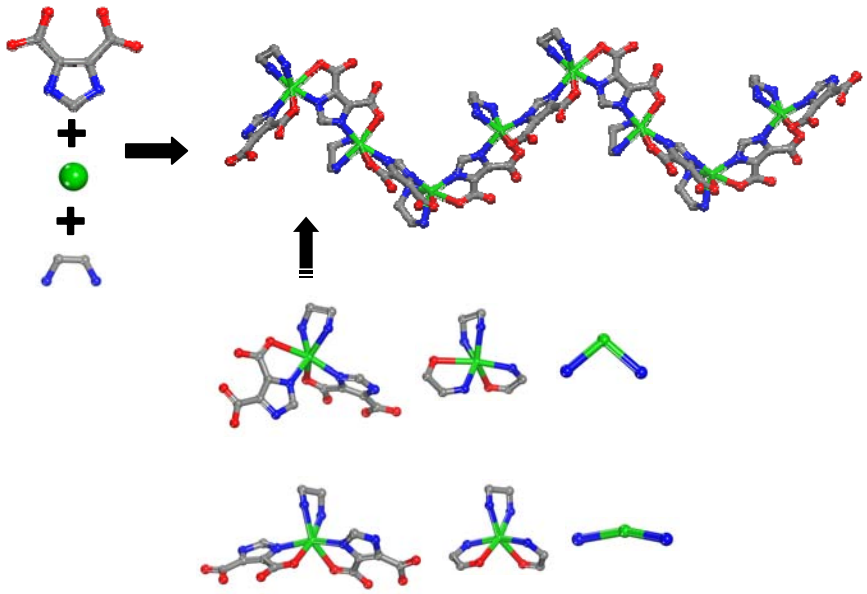

**Figure 3.7.** Two types of 2-connected MBBs combine to form zig-zag chains in ME089.

Another reaction condition containing 4,5-IMDC, cadmium, and ethylenediamine yielded interpenetrated 3-D nets, ME511, $\{[Cd(4,5\text{-IMDC})(en)]\}_n$. The single-metal ion is coordinated by two monodentate ethylenediamine bridges and two heterchelating 4,5-IMDC ligands in a *trans*-coordination and *trans*-chelation mode, to result in a neutral MOM. Each net is vertex transitive, with a Schlafi symbol of 4(2).8(4) and coordination sequence: 4, 10, 24, 44, 68, 98, 132, 172, 218, 266, which are identical to the chiral *uoc* net. The *uoc* net is isohedral, and the tile consists of 4- and 8MRs. The double interpenetration obstructs the 4- and 8MRs resulting in a densely packed framework. Once again, the unintentional coordination of ethylenediamine impedes structure

prediction. However, this serendipity allowed access to a framework previously uncommon in MOMs.

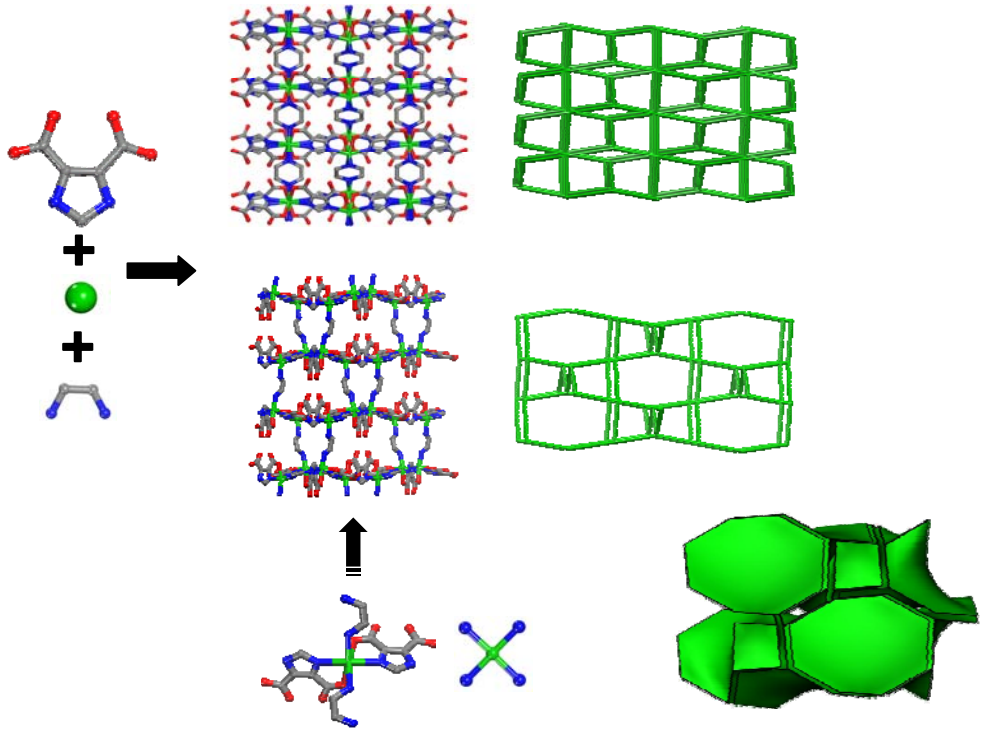

**Figure 3.8.** Doubly Interpenetrated *uoc* nets are constructed from a $MN_4O_2$ single-metal ion-based MBB, consisting of cadmium, 4,5-imidazolecarboxylate, and ethylenediamine.

Ethyl 4-imidazolecarboxylate (4-EIC) was reacted with cadmium in a solution of DEF and EtOH targeting an $CdN_4(CO_2)_2$ MBB, however an $CdN_4$ MBB resulted. The single-cadmium ion is coordinated by the nitrogen atom neighboring the carboxylate (Cd..N 2.25Å) in 4-EIC, while the 4-position nitrogen atom (Cd..N 2.19Å) further extends the neutral structure. When simplified into spacers and 4-connected nodes,

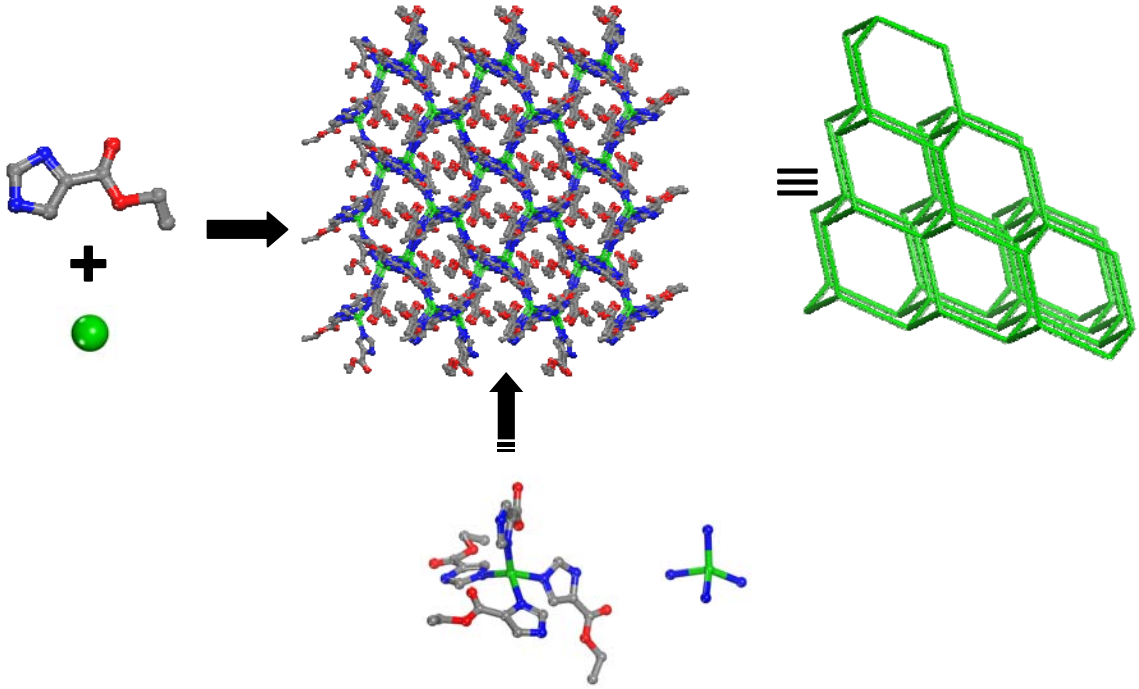

**Figure 3.9.** ME184, of *dia* topology, is constructed from a tetrahedral $CdN_4$ building block.

ME184 has *dia* topology, as exhibited by the 6(2).6(2).6(2).6(2).6(2).6(2) vertex symbol and 4, 12, 24, 42, 64, 92, 124, 162, 204, 252, 981 coordination sequence. Recent studies have proven that the MOF is stable in water, common organic solvents, and sodium hydroxide solutions at elevated and room temperatures.

### 3.3.2 MOMs from $MN_2O_4$ Single-Metal Ion-based MBBs

Reaction of 2,5-PDC and indium, in a 1:2 ratio, yielded a discrete metal-organic octahedron, $[In_6(2,5\text{-PDC})_{12}]$, ME694. The ditopic 2,5-PDC ligand heterochelates to the indium ion, while the 5-position carboxylate bridges resulting $InN_2(CO_2)_4$ MBBs, through monodentate coordination. As the nitrogen atoms, participating in heterochelation, and carboxylate oxygen atoms, coordinated in a monodentate fashion, direct the topology, the BU can be described as a distorted seesaw, in which the nitrogen atoms that constitute the fulcrum of the seesaw are have an approximate N-In-N bond angle of 154.5°. When the

distorted BU is combined with a ligand of ~120° angle, a MOP with octahedral geometry results.

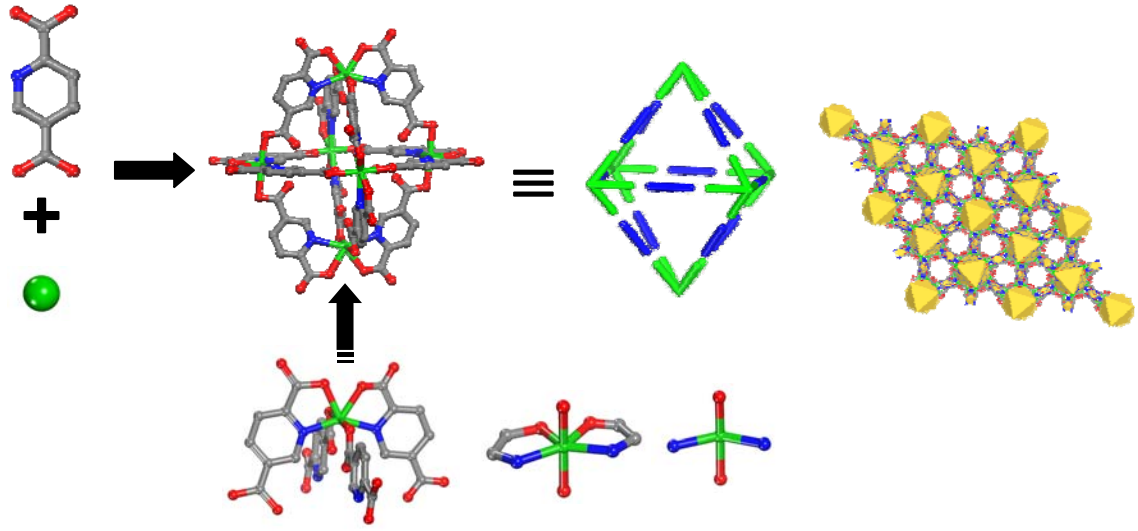

**Figure 3.10.** $[In_6(2,5\text{-}PDC)_{12}]$ consists of 4-connected MBBs with the formula $MN_2(CO_2)_4$.

Overall, six indium atoms and twelve ligand molecules are present in each of the discrete structures, encompassing an inner cavity with an approximate volume of 261Å$^3$, and a charge of -6 per octahedron. Each anionic polyhedron is accommodated by three piperazine guests, which bridge the structure, through hydrogen bonding, into three dimensions to result in small channels.

4-Imidazolecarboxylic acid (4-ICA) is used as a ditopic asymmetric ligand with one site of possible hetero-chelation and an additional nitrogen donor available for coordination to a metal ion. The angle between coordination sites in this ligand is 145° and used to target $MN_4(CO_2)_2$ MBBs.

A reaction of cadmium and 4-ICA, under solvothermal conditions, results in the generation of a 1-D zig-zag polymer, (ME096). This polymer contains MBBs which have a general formula $CdN_2(CO_2)_4$. The coordination spheres of

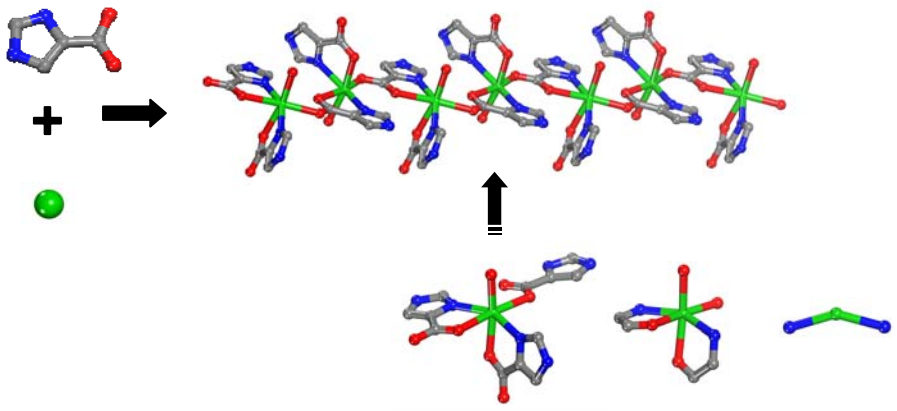

**Figure 3.11**. ME096 consists of zig-zag chains that are built from one type of MBB, composed of cadmium and 4-imidazolecarboxylic acid.

the cadmium metals are occupied by two ditopic linkers, one through chelation and the other through monodentate coordination, a water molecule and a chelating terminal 4-ICA ligand. Two coordinated donor atoms, the heterochelating nitrogen and the monodentate oxygen, are responsible for the topological outcome, resulting in a one dimensional chain. In contrast to what was targeted, the nitrogen in the 1 position of 4-ICA was not deprotonated and the ditopic linker was not coordinated through both nitrogen atoms of the ligand. Instead, only the 3-position nitrogen and the 4-position carboxylate oxygen atoms of 4-ICA coordinate to the cadmium center. Additionally, the neutral chains pack ABAB in a head to tail manner, to form layers. The layers pack ABAB and DMF guests reside between the layers.

Another solvothermally synthesized crystal, containing cadmium and 4-ICA**,** $\{[Cd(4\text{-}IMC)_2]\}_n$ (ME086), is constructed from a $CdN_2(CO_2)_4$ MBB. Each metal center

is coordinated by four ligands, two of which are monodentate oxygen atoms while the other two heterochelate through nitrogen and oxygen atoms the metal node, which results in a MBB with the formula $MN_2(CO_2)_4$. Once again, the 1-position nitrogen of 4-ICA was not deprotonated under these conditions, so the linker did not act as the 145° ditopic linker as expected, instead the bridging carboxylate further extend the structure into a 3-D MOM with *dia*-like topology. As mentioned earlier, the *dia* net is a regular net and thus highly expected when structure directing building blocks lack rigidity.

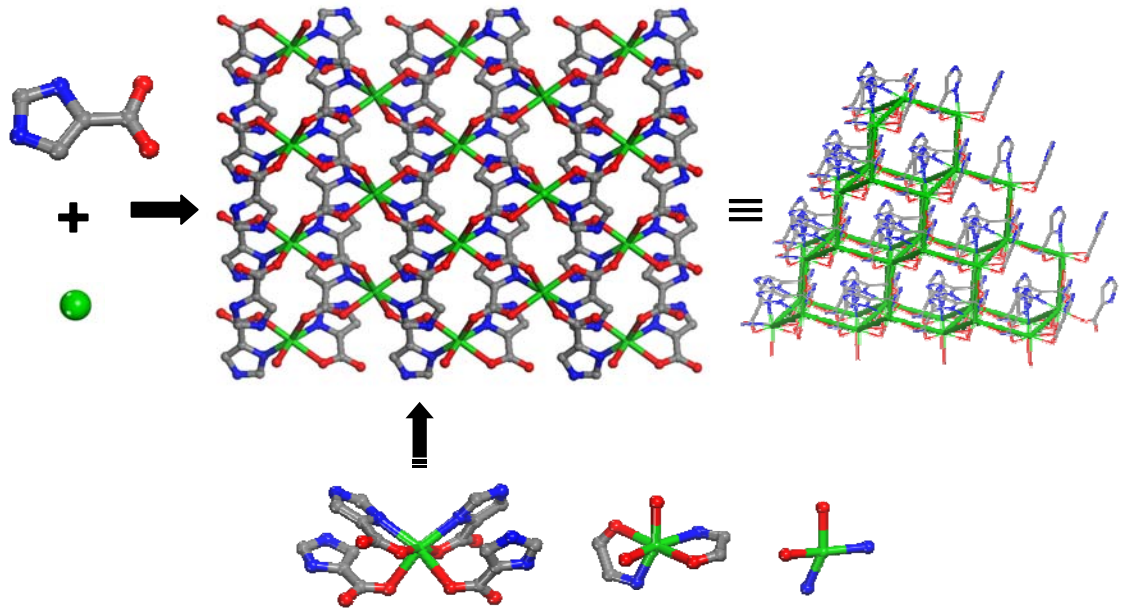

**Figure 3.12.** 4-IMC and cadmium ions are used to form a *dia* net from $MN_2(CO_2)_4$ MBBs.

It should be noted that ME096 and the ME086 can be assembled under the same reaction conditions under different temperatuers. When identical amounts of reagents are added to two different vials and one is heated at 85°C for 12 hours and the other is heated at 105°C for 23 hours ME096 and the ME086 are formed respectively. If the first vial containing ME096 is heated to 105°C the zig-zag chains are converted into the cubic diamond-like topology, ME086.

Previously, it has been proven feasible to synthesize assemblies that are isoreticular with indium-based assemblies, constructed from single-metal ion-based MBBs $MN_2(CO_2)_4$, using cadmium ions as the single-metal nodes in an instance where isoreticular metal-organic octahedra were produced with both metals. A 2-D cadmium-based framework (ME207) has been synthesized, using cadmium nitrate and 2,5-pyridinedicarboxylic acid, that is isoreticular with an indium-based Kagomé-like MOF.[2] In both cases, the $MN_2(CO_2)_4$ MBB results from nitrogen atoms coordinating in a *cis* fashion with rings of chelation that are 90° apart, which coincides with a $MN_2O_2$ BU.

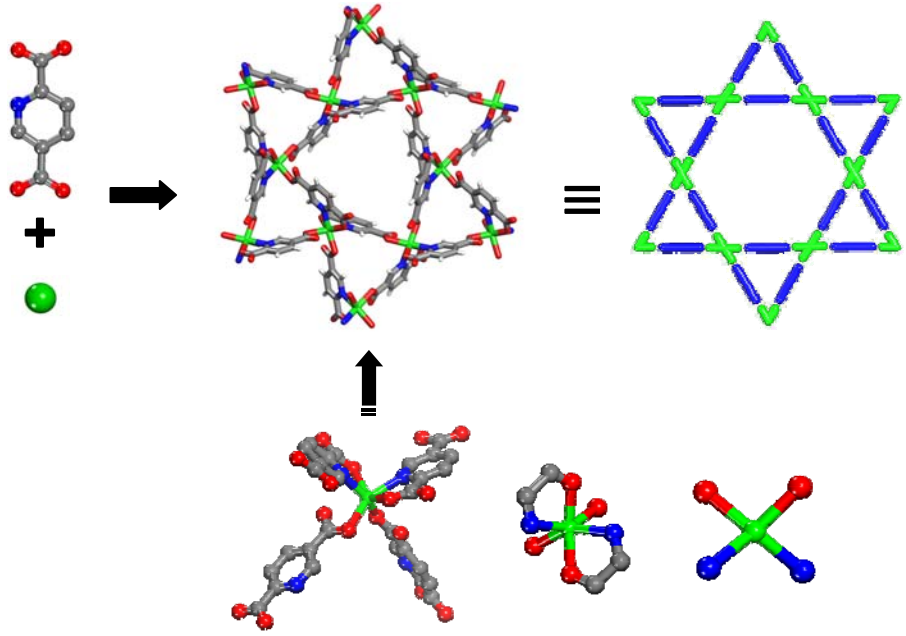

**Figure 3.13.** 2,5-PDC and cadmium ions can be used to construct a *kag* net from $MN_2O_2$ BUs resulting from $MN2(CO_2)_4$ MBBs

The crystal structure of ME207 contains large disordered guest molecules, which are likely imidazole and dimethylammonium cations to balance the anionic network, induced by from the 2:1 ratio of deprotonated $[2,5\text{-PDC}]^{2-}$ to $Cd^{2+}$ ions. The 2-D

Kagomé-like sheets stack relatively densely in an abcabc fashion, with no apparent channels.

### 3.3.3 MOMs Containing $MN_3O_3$ Building Units

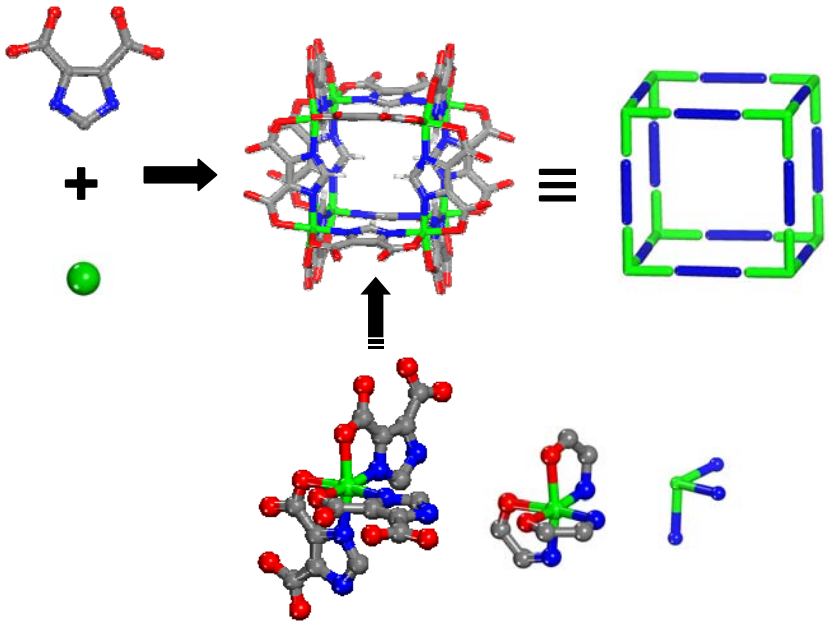

**Figure 3.14.** 4,5-IMDC and cadmium ions have been used to create a metal-organic cube from a *fac*-$MN_3(CO_2)_3$ MBB.

As mentioned earlier, the metal-nitrogen bonds of the *fac*-$MN_3(CO_2)_3$ MBB, the $MN_3$ BU, constitute the corner of a cube and can be employed in the edge-directed assembly of an anionic metal-organic cube.[73] It has since been proven that other single-indium metal ion-based MBBs can be synthesized with cadmium ions, and can be applied to recreate other single-metal ion-based MBBs, specifically using 4,5-IMDC as the heterchelating linker. A preliminary crystal structure of ME299 indicates that a nickel-based MOC has been recreated with cadmium nodes. As the versatile packing of MOCs can result in open or dense tertiary structures, this cadmium-based MOC exhibits cubic closest packing in an ABCABC fashion. Such packing results in a dense structure devoid of channels and cavities.

### 3.3.4 Heterocoordinated Metal-Organic Frameworks from MBBs

Nets based on one type of MBB are commonly crystallized, however, MOMs constructed from multiple types of MBBs can also be accessed. As the structures were unexpected, since the metals and ligands used are generally intended for the formation of predictable nets from one type of MBB, there is much to be learned from these examples. Such reaction conditions allowed the avoidance of envisioned nets *via* crystallization in topologies of higher transitivities. The focus will be nets containing 3- and 4-coordinate vertices.

Reaction of cadium acetate and 4,5-IMDC yields a 3-D MOF, JB9545, that is built from two 3- and one 4-connected MBBs. A tritopic 4,5-IMDC ligand, that coordinates through a monodentate nitrogen, N-, and O- heterochelation, and a monodentate oxygen connection. The other two MBBs are single-metal ion-based and

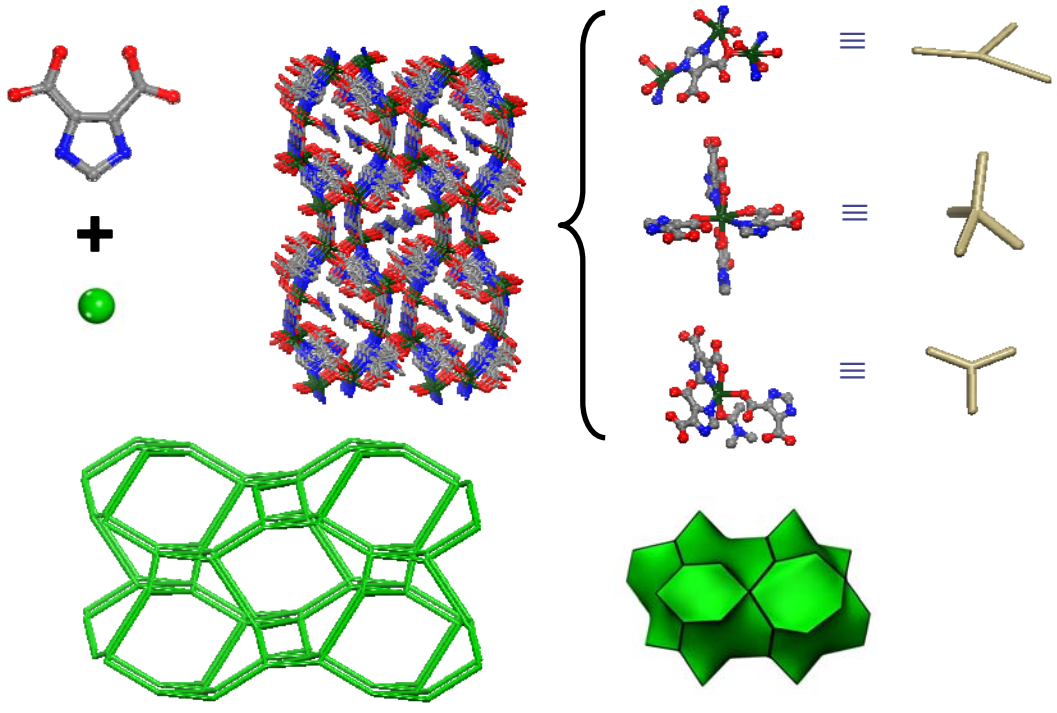

**Figure 3.15.** JB9545 is constructed from three types of MBBs yielding a net with unprecedented toplogy, which contains $[6^2.7^4.8^4.9^4]$ tiles.

related to previous examples. The 4-connected single-metal ion-based $CdN_2(CO_2)_4$ MBB, from a *trans*-$CdN_2O_4$ ion, exhibits *cis*-chelation and thus a see-saw-*like* BU, with nitrogen atoms in the fulcrum positions and oxygen atoms on the lever postions. The 3-connected $MN_2(CO_2)_3$ MBB consists of a single metal ion coordinated by three 4,5-IMDC ligands, two through N-, O-heterchelation and one through a monodentate oxygen connection, resulting in a trigonal planar BU. The sphere of coordination is completed by a terminal DMF or DMA molecule coordinated through a carboxylate oxygen atom.

Topologically, there are five different types of nodes, a metal-based 4-connected node (vertex symbol: 6.7.7.8.12(2)) and four different types of 3-connected nodes (vertex symbols: 6.7.8; 7(2).8.9(2); 7.7.8; 6.8.9(2)), of which two are ligand-based and two are metal-based, which composes an unprecedented topology, to the best of our knowledge. The net is tile transitive and is constructed two 6MRs, four 7MRs, four 8MRs, and four 9MRs. The networks consists of a two dimensional channel system from 6MRs, however, coordinated terminal ligands block access to the channels.

In another reaction between cadmium acetate and 4,5-IMDC an anionic, 3-D MOF with extra-large unidimensional channels was crystallized, namely, ME688. Two types of molecular building blocks. The $CdN_3(CO_2)_3$ MBB consists of three 4,5-IMDC ligands that heterochelate through N and O donor atoms, and the N atoms, in a facial arrangement, constitute and 3-connected BU. The $CdN_4$ MBB is formed through the coordination of four 4,5-IMDC ligands through nitrogen atoms, which can be viewed as a

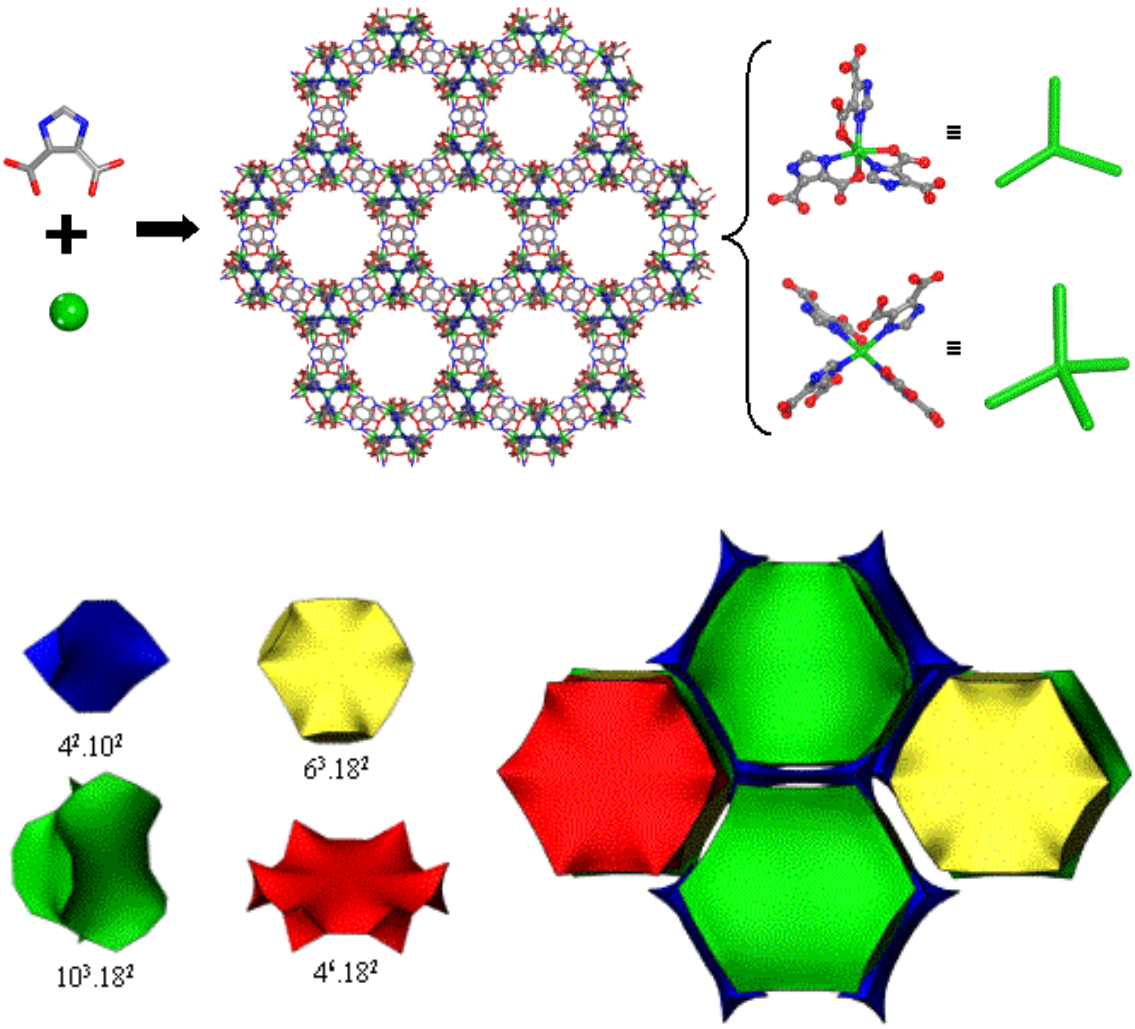


**Figure 3.16.** 4,5-IMDC and Cd are used to construct a (3,4)-net with unprecedented topology from two types of MBBs. The binodal network is built from four types of tiles.

tetrahedral BU. The 3-coordinate node has a coordination sequence of 3, 7, 11, 17, 28, 38, 52, 78, 92, 104, short (Schlafli) vertex symbol: 4.6.8, and long topological (O'Keeffe) vertex symbol: 4.6.10(4). The 4-coordinate node has a coordination sequence 4, 6, 11, 20, 26, 40, 60, 70, 91, 116, short (Schlafli) vertex symbol: 4(2).6.8(2).10, and long topological (O'Keeffe) vertex symbol: 4.4.6.10(4).10(2).10(2). In this unprecedented net, the 3- and 4-coordinate nodes facilitate the formation of 4-, 6-, and 10-MRs with

accessible windows of approximately 2.75, 7.7, and 6.5 x 18.6Å, respectively. The 4-, 6-, and 10MRs constitute the walls of unidimensional channels with an approximate diameter of 15 Å along the z-axis, while smaller channels are accessible through the x- and y-axes. This open anionic material is capable of ion-exchange of large organic molecules, such as acridine yellow (Appendix III).

These examples show that MBBs based on heterochelating ligands can be used to access MOFs with heterocoordination, or mixed types of nodes. Although these types of nets are challenging to predict and/or construct from design, these occurrences allow insights to capabilities and further design advancements.

## 3.4 Summary & Conclusions

This class of compounds illustrates that varied modes of heterochelation combined with ligand angularity directs the formation of numerous nets. Overall,

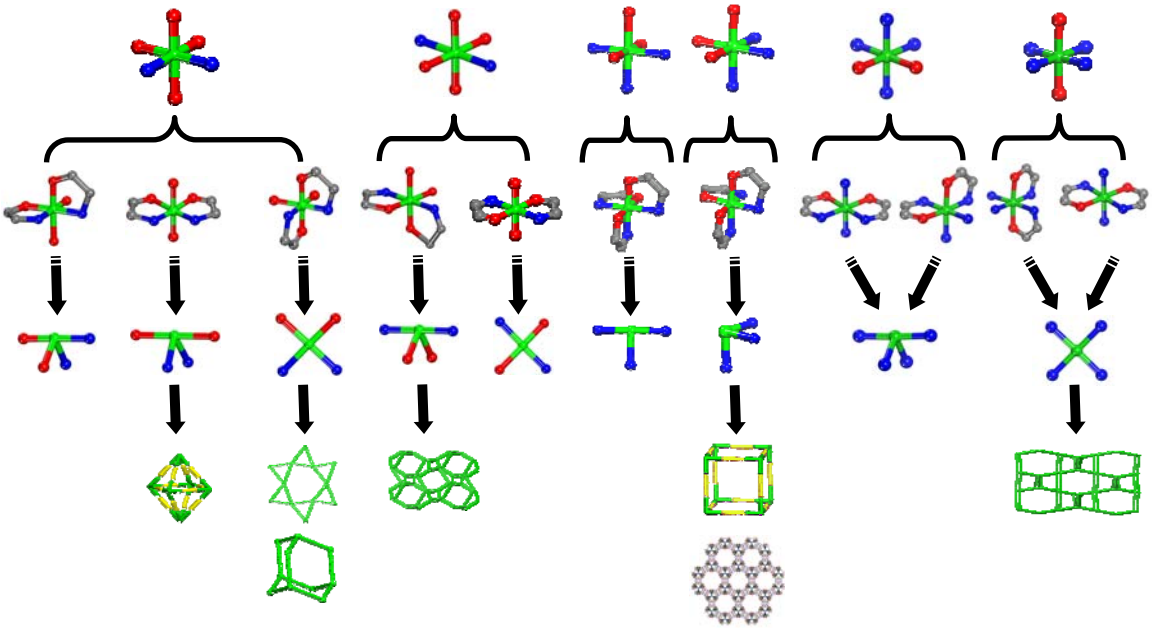

**Figure 3.17.** Molecular building blocks, constructed from $MN_xO_y$ ($x + y = 6$) single-metal ions can facilitate the formation of various metal-organic materials.

combining the approaches of nitrogen-based and carboxylate-based ligands, which exploit hetero-chelation involving nitrogen and oxygen, in the deliberate synthesis of MOFs from single-metal-ion-based MBBs, is an effective method of synthesizing discrete and extended metal-organic assemblies. Thus far, certain MBBs, and consequential BUs, predominate and dictate the formation of certain structures. Exploration of advancing this approach to other metal coordination modes, $MN_x(CO_2)_y$, and discovering common conditions to formulate projected frameworks will continue to advance the design of such materials.

## Chapter 4: Design of Zeolite-*like* Metal-Organic Frameworks

Zeolites are currently the largest class of commercially available functional porous materials. Zeolites are classically defined as exclusively aluminosilicate, three-dimensional, open frameworks consisting of corner-sharing $[AlO_4]^{5-}$ and $[SiO_4]^{4-}$ tetrahedra with the general formula $M^{n+}_{x/n}[(AlO_2)_x(SiO_2)_y]^{x-} \bullet w\ H_2O$, capable of ion exchange and reversible dehydration.[80] Naturally occurring zeolites have been studied for over 200 years, while research of the synthesis of zeolites has been progressing for over 140 years.[81] Zeolites, which have high thermal stabilities, can contain multidimensional as well as unidimensional pore systems, or channels. The pores have molecular dimensions and are able to accommodate small guest molecules. Although unidimensional pore systems are appropriate for some applications, the bulk of zeolitic research is focused on frameworks consisting of multidimensional pore systems.

Zeolite research is captivating due to a variety of applications, including catalysis, ion exchange, gas storage, purification and separation, etc.[82] mainly resulting from permanent porosity and intrinsic declination of interpenetration. Specific applications include recovery of radioactive ions from waste solutions,[83] separating hydrogen isotopes, solubilizing enzymes, carrying active catalysts in the curing of plastics and rubber, transporting soil nutrients in fertilizers, hydrocarbon conversion catalysis,[84-85] and silicon nanowire synthesis.[86] Zeolites have proven futile for some applications, such as methane storage, separation/catalysis of large molecules, molecular magnetism, and hydrogen storage.

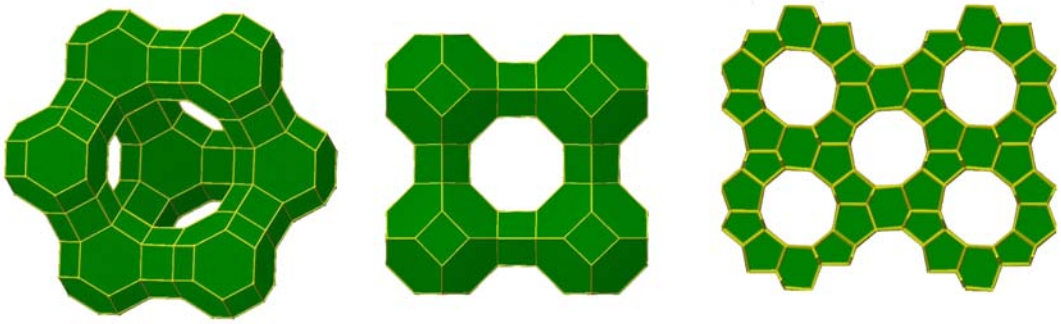

**Figure 4.1.** A few zeolite frameworks are illustrated to display the porous nature of the naturally occurring aluminosilicate compounds. *left*: faujasite (*fau*) *center*: Linde Type A (*lta*) *right*: $AlPO_4$-5 (*afi*)

Zeolites are commercially used for ion exchange.[82,84,87] The presence of aluminum in the silicate lattice induces a negative charge within the framework. The anionic framework is compensated by cationic guests that are present within the pores or channels. These intrinsic anionic properties allow ion-exchange to occur, which highly impacts possible commercial applications. The capacity for reversible cation-exchange is very important in zeolites because it allows manipulation of the electronic atmosphere inside pores. Sorption properties are dependant on the cations present within the cavities. For example, when the sodium cations present in the pore system of the zeolite Linde Type A (*lta*) are replaced with potassium cations the sorption capacity for oxygen is essentially eliminated. It is also apparent that propane is not sorbed by the *lta* zeolite that contains sodium, however, when the sodium ions are exchanged with calcium, *lta* is capable of propane sorption. Cation-exchange in zeolites is also influential on catalytic properties and separation capabilities.[84]

An arduous objective is to increase pore sizes of multidimensional channel systems of zeolite-like materials and design frameworks that possess tunable properties and novel functionalities that exceed the boundaries of currently available porous

materials. The potential for design of MOMs offers a means to expand zeolitic frameworks and thus further develop applications based on solid-state materials.

## 4.1 *Zeolite-like* Metal-Organic Frameworks from Supermolecular Building Blocks

The ability to control coordination number, and thus geometry, around metal nodes through metal-ligand directed assembly affords the synthesis of pre-designed finite and rigid metal-organic polyhedra (MOPs).[4,23,67,73,88] MOPs with peripheral functionalities can be employed further as supermolecular building blocks (SBBs) in the construction of extended metal-organic frameworks (MOFs).[89-90] This approach is illustrated in the construction of *rht*-MOF, in which a metal-organic nanoball (cubohemioctahedron) is peripherally functionalized with tetrazole groups that form a trimeric metal cluster. Essentially, the network is synthesized using 5-tetrazolylisophthalic acid and copper nitrate. Just as the cubohemioctahedron can be functionalized and, thus, extended, various other MOPs with appropriately placed points of extension can be used as augmented versions of defined nodes with high connectivity. Programming such building blocks with a hierarchy of appropriate information to promote the synthesis of targeted structures, while simultaneously avoiding other easily attainable nets,[91] represents a significant advancement in framework design.[28]

In crystal chemistry edge transitive nets are suitable targets for such processes, since they are simple networks composed from only one kind of edge. Our pre-designed finite metal-organic cube MOC[73] can be employed as a rigid and directional SBB for the directed assembly and deliberate construction of extended MOFs based on 8-connected edge transitive nets. According to the RCSR,[50] only five 8-connected nets are edge

transitive, *bcu, bcu-b, lcx, reo,* and *thp*. Of these basic nets, *bcu* and *reo* are closely related to zeolite nets, specifically, the augmentation of the 8-connected nodes result in zeolite nets *aco* and *lta*.

A particular subset of zeolite nets share a common secondary building unit (SBU) composed of eight tetrahedra bridged through oxide ions in a cube-like arrangement, commonly referred to as a double 4-ring, d4R.[81] The analogy of this SBU to a cube (and, by default, a MOC) suggests that MOCs could be used as SBBs to target zeolite nets based on d4Rs.

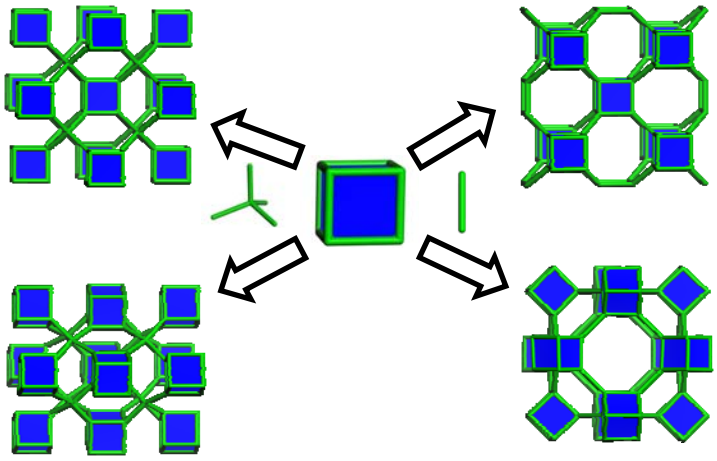

**Figure 4.2.** *ast, aco, asv,* and *lta* are zeolitic nets closely related to basic 8-connected nets, and thus exceptionally interesting to metal-orgaic crystal chemistry.

Our approach encompasses using MOCs as 8-connected building blocks, which can be regarded as d4Rs to construct ZMOFs related to 8-connected edge-transitive nets. The d4Rs can be connected through linear linkers to construct zeolite-like nets.

As previously described, a metal-organic molecular cube can be assembled through hetero-chelation of octahedral single-metal ions by ditopic bis-bidentate linkers in a *fac*-$MN_3(CO_2)_3$ manner,. The molecular cube itself consists of eight vertices

occupied by tri-connected nodes bridged through twelve 4,5-imidazoledicarboxylate ($H_n$ImDC, $n$ = 0-1) linkers. By the coordination of such vertices, interconnected tetrahedra similar to the D4R units in zeolites can be attained. The MOCs possess peripheral carboxylate oxygen atoms that can potentially coordinate additional metal ions and/or participate in hydrogen bonding to construct ZMOFs.

### 4.1.1 Experimental

All chemicals were used as received from Fisher Scientific, Sigma-Aldrich, and TCI America chemical companies. Fourier transform infrared (FT-IR) spectra were measured using an Avatar 320 FT-IR system. Absorptions are described as follows: very strong (vs), strong (s), medium (m), weak (w), shoulder (sh), and broad (br). X-ray powder diffraction (XRPD) data were recorded on a Rigaku RU15 diffractometer at 30kV, 15mA for $Cu_{K\alpha}$ ($\lambda$ = 1.5418 Å), with a scan speed of 1°/min and a step size of 0.05° in 2θ. Calculated XRPD patterns were produced using PowderCell 2.4 software. Single-crystal X-ray diffraction (SCD) data were collected on a Bruker SMART-APEX CCD diffractometer using $Mo_{K\alpha}$ radiation ($\lambda$ = 0.71073 Å) operated at 2000 W power (50 kV, 40 mA). The frames were integrated with SAINT software package[74] with a narrow frame algorithm. The structure was solved using direct methods and refined by full-matrix least-squares on $|F|^2$. All crystallographic calculations were conducted with the SHELXTL 5.1 program package,[75] and performed by Dr. Victor Kravtsov, Dr. Lukasz Wojtas, Dr. Derek Beauchamp, Dr. Rosa Walsh or Gregory J. McManus in the Department of Chemistry at the University of South Florida. Crystallographic tables are included for each compound in Appendix I

Olex[76] and Topos[77] software was used to determine topological representations of the obtained MOMs, and the resulting terms compared to those in the literature and the RCSR database.[50] All total solvent-accessible volumes were determined using PLATON[78] software by summing voxels more than 1.2 Å away from the framework. Tiling was evaluated using 3dt software.[79]

**Synthesis of $C_{634}H_{414}N_{234}O_{807}Cd_{72}Na_{72}$, ME500**. $H_3$ImDC (0.087 mmol, 13.6 mg), $Cd(NO_3)_2{\cdot}4H_2O$ (0.0435 mmol, 13.4 mg), N,N'-diethylformamide (1 ml), ethanol (0.25 ml), piperazine (0.1 ml, 0.58 M in DMF), sodium hydroxide (0.1 ml, 0.174 M in ethanol), and 2,4-pentanedione (0.1 ml, 0.174 M in ethanol) were added to a 25 ml scintillation vial, which was then sealed, heated to 85˚C and cooled to room temperature at a rate of 1˚C/min to produce colorless, hexagonal prism-like crystals formulated as $C_{634}H_{414}N_{234}O_{807}Cd_{72}Na_{72}$ with a 67% (0.0137 g) yield based on ?. FT-IR (4000–600 $cm^{-1}$): 1650.25 (w), 1622.59 (w), 1548.82 (s), 1484.49 (vs), 1437.5 (s), 1379.16 (s), 1298.34 (m), 1253.75 (m), 1217.09 (w), 1110.98 (m), 997.18 (w), 975.02 (w), 846.39 (w), 786.95 (s), 667.49 (vs), 655.87 (vs), 613.00 (s)

### 4.1.2 Results & Discussion

Reaction of $Cd(NO_3)_2.4H_2O$ and $H_3$ImDC in the presence of $Na^+$ ions results in *lta*-ZMOF, formulated as $\{[Cd_8(HImDC)_8(ImDC)_4](H_2Pip)_2Na_8(EtOH)_5(H_2O)_{37}\}$ (Pip=Piperazine, EtOH=Ethanol). In the crystal structure of *lta*-ZMOF, each MOC is linked to eight other cubes through linear vertex-to-vertex connections. Half are connected through hydrogen bonded water molecules and the other four vertices are connected through a series of four sodium atoms, Figure 4.3. The framework consists of

two types of cages, namely an α-cage encapsulated by 12 cubes and an elliptical β-cage enclosed by 6 cubes. The largest sphere that can fit into these cages without touching the van der Waals surface of the framework is ~32 Å for the α-cage and ~8.5 Å for the β-

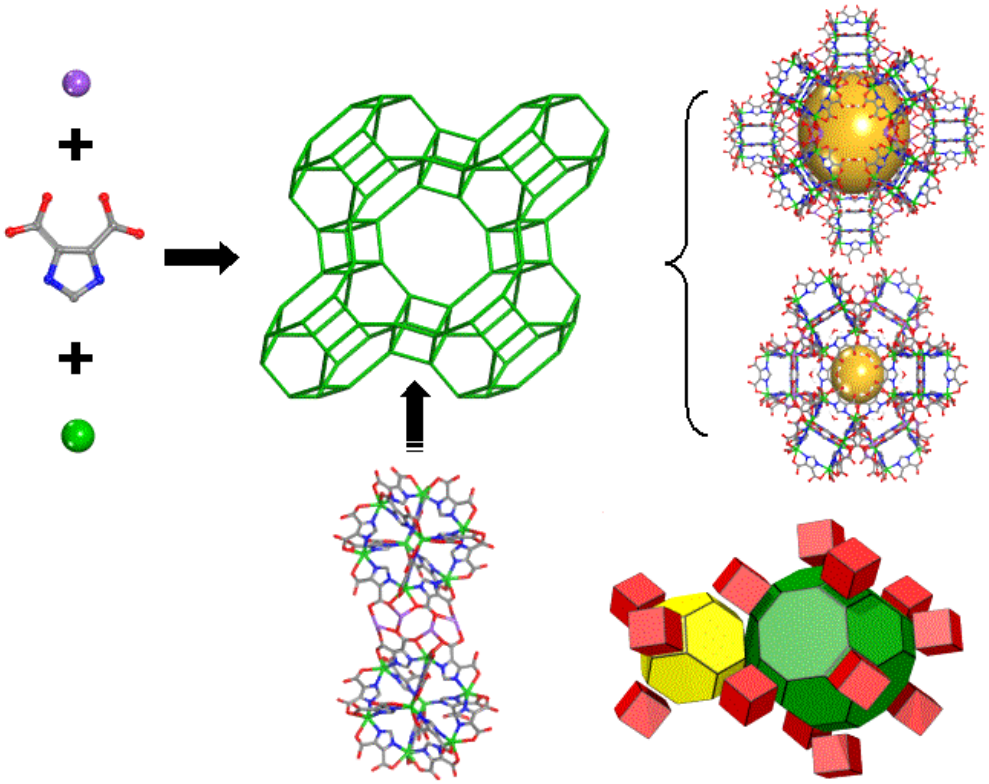

**Figure 4.3.** In *lta*-ZMOF, twelve MOCs are connected through a series of sodium ions (top left) to generate an α-cage (tile shown in green) that can accommodate a sphere with diameter of ~32 Å and 6 MOCs assemble a β-cage (tile shown in yellow) that can fit a sphere of ~8.5 Å in diameter.

cage. Topologically, the framework can be viewed as *lta* or an augmented version of *reo* when the hydrogen bonded and sodium bridged vertex-vertex connections are considered. However, the structure can be interpreted as *nbo* if only connections through sodium ions are considered.

This work demonstrates that utilization of MOPs as SBBs represents an interesting approach towards rational design and synthesis of nanostructures. MOCs, the

MOPs of significance, offer the potential to target and build zeolitic frameworks containing d4Rs. The aforementioned SBBs contain a hierarchy of information regarding the evolution of single metal ions, with anticipated coordination geometries, deemed as rigid and directional vertices, via heterochelation, into MOPs that can be used as defined high-connected building blocks to yield zeolitic frameworks.

## 4.2 Zeolite-*like* Metal-Organic Frameworks from $MN_x(CO_2)_y$ Molecular Building Blocks

To date, $MN_4O_4$, $MN_4O_2$,[65, 92] and $MN_4$[51] MBBs have been observed in metal-organic zeolite-like materials constructed from imidazole- or pyrimidine-based linkers. Consistently, in all cases the TBUs are of the general formula $MN_4$ in which the nitrogen atoms direct the topology. It is conceivable that the points of extension in the tetrahedron can be interchanged with atoms, other than nitrogen, in an aim to target nets uncommon in metal-organic crystal chemistry. $MN_4O_2$ and $MN_4O_4$ MBBs, which correspond to $MN_4$ TBUs, have been built from 8- and 6-coordinate metal nodes, respectively, and ligands that form 5MR of heterochelation to the metal center through nitrogen and carboxylate-oxygen atoms. Additionally, $MN_2O_4$ MBBs, from 6-coordinate metals, predictably form $MN_2O_2$ TBUs in which two nitrogen atoms (participating in heterchelation) and two monodentate oxygen atoms direct the topology. To facilitate the formation of such TBUs, it is desirable to avoid MBBs that solely consist of heterochelation and/or monodentate nitrogen coordination. Therefore, when scheming the heterochelating ligand that forms $MN_2O_2$ building units, an assymetric ditopic ligand with a site appropriate for N-, O-heterchelation and a bridging carboxylate group is appropriate. When the $MN_2O_2$ TBUs are intended to be used to construct ZMOFs, the

angle through which they are connected will ideally correspond to the optimal T-O-T bonding angles exhibited in traditional zeolites, as is 2,4-Pyridinedicarboxylic acid (2,4-$H_2$PDCA).

### 4.2.1 Experimental

All chemicals were used as received from Fisher Scientific, Sigma-Aldrich, and TCI America chemical companies. Fourier transform infrared (FT-IR) spectra were measured using an Avatar 320 FT-IR system. Absorptions are described as follows: very strong (vs), strong (s), medium (m), weak (w), shoulder (sh), and broad (br). X-ray powder diffraction (XRPD) data were recorded on a Rigaku RU15 diffractometer at 30kV, 15mA for $Cu_{K\alpha}$ ($\lambda$ = 1.5418 Å), with a scan speed of 1°/min and a step size of 0.05° in 2$\theta$. Calculated XRPD patterns were produced using PowderCell 2.4 software. Single-crystal X-ray diffraction (SCD) data were collected on a Bruker SMART-APEX CCD diffractometer using $Mo_{K\alpha}$ radiation ($\lambda$ = 0.71073 Å) operated at 2000 W power (50 kV, 40 mA). The frames were integrated with SAINT software package[74] with a narrow frame algorithm. The structure was solved using direct methods and refined by full-matrix least-squares on $|F|^2$. All crystallographic calculations were conducted with the SHELXTL 5.1 program package,[75] and performed by Dr. Victor Kravtsov, Dr. Lukasz Wojtas, Dr. Derek Beauchamp, Dr. Rosa Walsh or Gregory J. McManus in the Department of Chemistry at the University of South Florida. Crystallographic tables are included for each compound in Appendix I

Olex[76] and Topos[77] software was used to determine topological representations of the obtained MOMs, and the resulting terms compared to those in the literature and the RCSR database.[50] All total solvent-accessible volumes were determined using

PLATON[78] software by summing voxels more than 1.2 Å away from the framework. Tiling was evaluated using 3dt software.[79]

**Synthesis of $\{In(2,4\text{-}PDC)_2]\}_n$, ME654**: A solution of $In(ac)_3H_2O$ (0.0435 mmol) and 2,4-PDC (0.087 mmol) in 1 mL of DEF, 0.5mL of ethanol, and 0.1mL of 1M tetrabutylammonium sulfate in water was prepared. The solution was then heated to 85°C for 12 h, pure colorless crystals were obtained. FT-IR (4000-600 $cm^{-1}$): 3386(br), 3109(br), 2350(m), 1653(s), 1600(m), 1485(m), 1431(s), 1380(vs), 1248(s), 1100(s), 1057(s), 785(s), 754(s), 727(vs), 657(s), 614(s).

**Synthesis of $\{In(2,4\text{-}PDC)_2]\}_n$, ME658**: A solution of $In(ac)_3H_2O$ (0.0435 mmol) and 2,4-PDC (0.087 mmol) in 1 mL of DMA, 0.5mL of ethanol, and 0.1mL 1.6M diethylamine in DMF was prepared. The solution was then heated to 85°C for 12 h, pure colorless crystals were obtained. FT-IR (4000-600 $cm^{-1}$): 3386(br), 3109(br), 2350(m), 1653(s), 1600(m), 1485(m), 1431(s), 1380(vs), 1248(s), 1100(s), 1057(s), 785(s), 754(s), 727(vs), 657(s), 614(s).

### 4.2.2 Results & Discussion

Overall, combining the approaches of nitrogen-based and carboxylate-based ligands, in the deliberate synthesis of MOFs, into single-metal-ion-based MBBs, which exploit heterochelation involving nitrogen and oxygen, is an effective method of synthesizing discrete and extended metal-organic assemblies. Thus far, certain MBBs, and consequential SBUs, predominate and dictate the formation of certain structures. Exploration of advancing this approach to other metal coordination modes, $MN_x(CO_2)_y$,

and discovering common conditions to formulate projected frameworks from specific MBBs is currently under development. Herein, two novel ZMOFs constructed from 2,4-PDC and Indium, namely *ana*-ZMOF and *sod*-ZMOF-1 are presented.

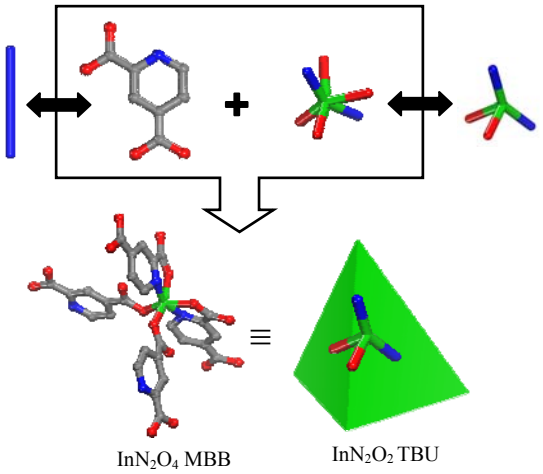


**Figure 4.4.** An $MN_2(CO_2)_4$ molecular building block can be exploited as an $MN_2O_2$ tetrahedral building unit.

In crystal design, the formation of regular nets is common, and sometimes unavoidable. Furthermore, of zeolite nets, those with higher regularity are reasonable targets. While there are no regular or quasiregular zeolite nets, sodalite and analcime are the only two examples of zeolitic nets that are semiregular. Sodalite and analcime have transitivities of 1121 and 1132, respectively. Both structures consist of one type of vertex (vertex transitive) and one type of edge (edge transitive). Additionally, these nets are the only edge transitive zeolite nets. Such regularity deems sod- and ana- nets as suitable targets in crystal chemistry, and due to the tile-transitivity of *sod,* it is especially plausible.

The *ana* net consists of irregular 3-dimensional channels formed by highly distorted 8MRs, and is composed of two types of tiles, one with two hexagonal and three

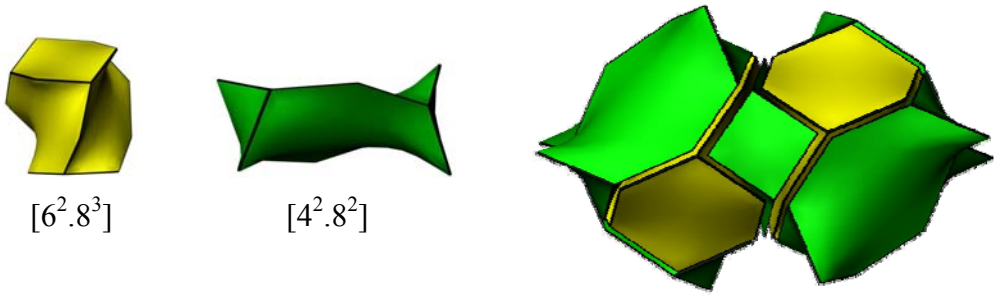


**Figure 4.5.** Tiles of *ana* net are constructured from two hexagons, three octagons (yellow), and two quadrangles and two octagons (green).

octagonal faces and the other from two tetragonal and two octagonal faces. In *ana*-ZMOF, $InN_2O_2$ BUs replace tetrahedral atoms of inorganic analcime, and are linked through the doubly deprotonated bridging ligand, 2,4-pyridinedicarboxylate (2,4-PDC), which is an expansion of the oxygen bridges of T-O-T in zeolites. The resulting anionic structure has dimensions appropriate for ion-exchange of large organic cations, such as acridine yellow (Appendix III).

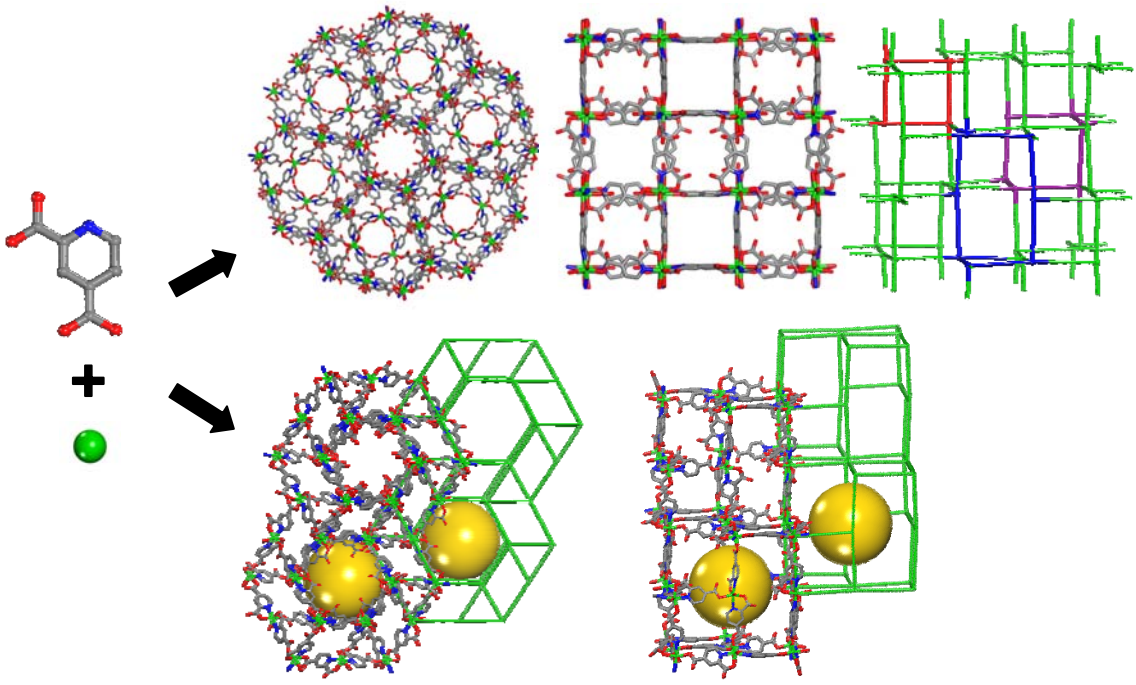

**Figure 4.6.** 2,4-PDC and indium ions can be used to construct ZMOFs related to *ana* and *sod* nets.

In the structure of *sod*-ZMOF(1) the sodalite net is assembled from highly distorted β-cages built from 4MRs and planar and chair-like 6MRs, and the distortions allow for the encapsulation of larger molecules than analogues with regular cages. For example, a sod-ZMOF constructed from $In^{3+}$ and 4,6-pyrimidinedicarboxylate,[92] with regular cages, has proven capable of exchanging small inorganic cations, however, is resistant to the adsorption of larger acridine molecules. This comparison provides evidence that by altering just one atom of a ligand, the atoms/points of extension of the building unit can be controlled, and the properties of the resultant material can be delicately tuned.

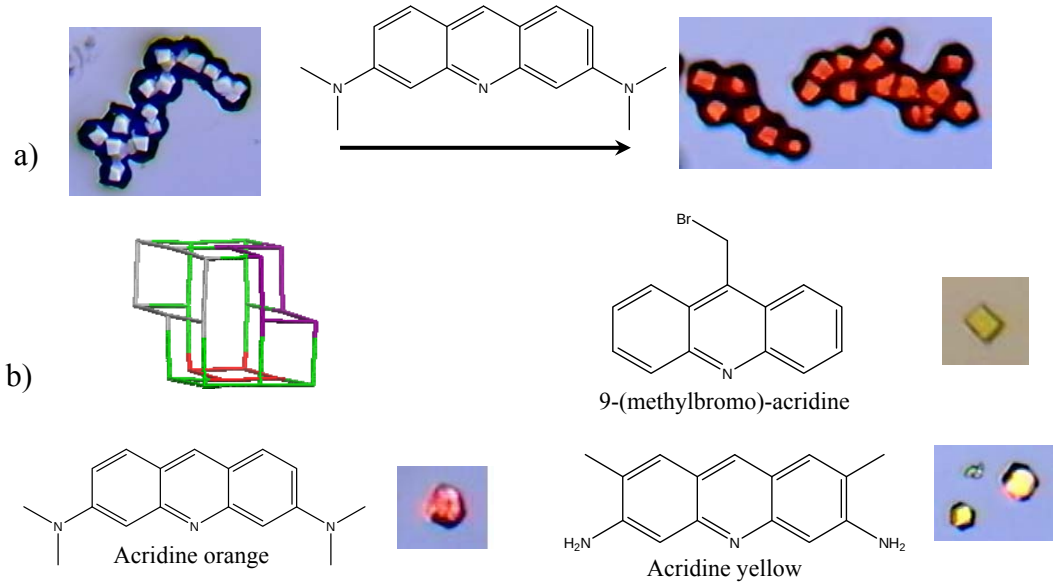


**Figure 4.7.** a) optical images of ion-exchange in *ana*-ZMOF with acridine orange. b) optical images of ion-exchange in *sod*-ZMOF.

### 4.3 Zeolite-*like* Metal-Organic Frameworks Organic Tetrahedral Nodes

Metal-organic tetrahedral building units (TBUs) can be connected through appropiate angles to faciliate the expansion of the Si/Al nodes and oxide atom ($O^{2-}$) bridges of zeolites and, ultimately lead to non-interpenetrated, enlarged, multidimensional pore systems and/or cavities. Our group, among others, has demonstrated that metal-organic TBUs can be designed and exploited in the construction of various ZMOFs.[65,92] In an effort to extend this innovation to other unprecendented ZMOFs, we deliberate the use of purely organic TBUs. Previously, HMTA, containing accessible N-donor atoms in a tetrahedral arrangement, has been deemed as an appropriate TBU. The remaining resulting challenge is to utilize metal coordination to bridge the TBUs at an angle analogous to the bonding angle of $O^{2-}$ found in zeolites.

Organic ligands can be selected to induce directionality in framework design. For instance, hexamethylenetetramine (HMTA) contains nitrogen atoms in a tetrahedral arrangement that can be utilized to position coordinated metals at approximate 109.5° angles. Additionally, metals of high coordination can be employed as 2-connected linkers while small terminal ligands, such as acetate and water, can complete the sphere of coordination. Exploration of reaction conditions involving such variables can lead to the realization of networks, constructed from organic tetrahedral nodes, with tunable ionic strength and interesting topologies. Previously, hexamethylenetetramine (HMTA), containing N-donor atoms in a tetrahedral arrangement, has been deemed as a suitable TBU. The remaining challenge is to utilize metal coordination, as a function of auxiliary ligands, to bridge the TBUs at an angle analogous to the bonding angle of $O^{2-}$ found in zeolites.

Cadmium ($Cd^{2+}$) has previously exhibited the desired bond angle, when coordinated by HMTA, to assemble a net with *mtn*-like topology.[93] In this example, HMTA ligands coordinate to the axial postions of each cadmium ion and three equatorial positions are occupied by water molecules, resulting in a cationic network. It is feasible that replacement of the water molecules with other small, terminal ligands assists in slight variations of appropriate N-Cd-N bond angles to achieve an assortment of zeolite-*like* topologies. Additionally, the charge of the framework can be controlled by varying the ionic nature of the selected auxiliary ligands. Whereas three auxiliary water ligands yielded a cationic framework, systematic replacement with anionic ligands can produce cationic, neutral or anionic frameworks. As the ionic nature of the framework can be controlled, ionic structure directing agents can be varied to access unprecedented

ZMOFs. Herein, a rare coordination sphere of cadmium is occupied by three equatorial acetate ions and two nitrogen atoms in the axial positions, from HMTA ligands, to construct three anionic ZMOFs. The acetate anions simultaneously complete the coordination sphere of the cadmium linker, allow the formation of suitable N-Cd-N bond angles, and contribute to the ionic nature of the framework, which may be exploited in ZMOF design. Reaction conditions for the synthesis of anionic *mep*-ZMOF, using HMTA as an organic TBU and a cadmium ion as an angular linker, was fortuitously discovered. Consequently, it was determined that varying cationic structure directing agents (SDAs), under similar conditions, allowed consistant access to appropriate N-Cd-N angles, and ultimately unprecedented ZMOFs related to *sod* and *mtn* topologies.

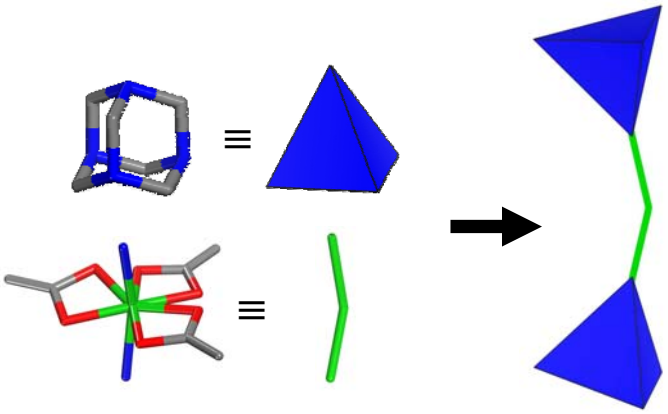

**Figure 4.8.** The nitrogen atoms (blue) of hexamethylenetetramine, situated in a tetrahedral arrangement, can coordinate to metal ions to act as a tetrahedral building unit, and, when connected through appropriate angles (as shown in green), can facilitate the formation of zeolite-*like* metal-organic frameworks.

### 4.1.1 Experimental

All chemicals were used as received from Fisher Scientific, Sigma-Aldrich, and TCI America chemical companies. Fourier transform infrared (FT-IR) spectra were measured using an Avatar 320 FT-IR system. Absorptions are described as follows: very strong

(vs), strong (s), medium (m), weak (w), shoulder (sh), and broad (br). X-ray powder diffraction (XRPD) data were recorded on a Rigaku RU15 diffractometer at 30kV, 15mA for $Cu_{K\alpha}$ ($\lambda$ = 1.5418 Å), with a scan speed of 1°/min and a step size of 0.05° in 2θ. Calculated XRPD patterns were produced using PowderCell 2.4 software. Single-crystal X-ray diffraction (SCD) data were collected on a Bruker SMART-APEX CCD diffractometer using $Mo_{K\alpha}$ radiation ($\lambda$ = 0.71073 Å) operated at 2000 W power (50 kV, 40 mA). The frames were integrated with SAINT software package[74] with a narrow frame algorithm. The structure was solved using direct methods and refined by full-matrix least-squares on $|F|^2$. All crystallographic calculations were conducted with the SHELXTL 5.1 program package,[75] and performed by Dr. Victor Kravtsov, Dr. Lukasz Wojtas, Dr. Derek Beauchamp, Dr. Rosa Walsh or Gregory J. McManus in the Department of Chemistry at the University of South Florida. Crystallographic tables are included for each compound in Appendix I

Olex[76] and Topos[77] software was used to determine topological representations of the obtained MOMs, and the resulting terms compared to those in the literature and the RCSR database.[50] All total solvent-accessible volumes were determined using PLATON[78] software by summing voxels more than 1.2 Å away from the framework. Tiling was evaluated using 3dt software.[79]

**Synthesis of *mep*-ZMOF:** $Cd(Ac)_2{}^{\bullet}H_2O$ (0.104g, 0.3915mmol), hexamethylenetetramine (0.100 g, 0.713mmol), DEF (2.25mL), ethanol (0.50mL) were combined in a 20-mL vial, which was sealed and heated to 85˚C for 12h, 105˚C for 23h and then cooled to room temperature. Colorless polyhedral crystals were collected and air dried, yielding 0.0657g

FT-IR: 3308.92 (br), 2970.32 (m), 1657.01 (w), 1558.4 (s), 1417.75 (s), 1380.15 (s), 1232.11 (s), 1161.98 (w), 1130.1 (w), 1049.8 (w), 1001.39 (vs), 951.89 (m), 815.3 (s), 671.29 (s), 620.41 (s)

**Synthesis of *sod*-ZMOF(2):** $Cd(Ac)_2 \bullet H_2O$ (0.052g, 0.19575mmol), hexamethylenetetramine (0.050 g, 0.357mmol), DMA (1.125mL), ethanol (0.125mL), water (0.25mL) tetramethylammonium nitrate (0.05mL, 1M in $H_2O$) were combined in a 20-mL vial, which was sealed and heated to115˚C for 23h and cooled to room temperature. Colorless polyhedral crystals were collected and air dried, yielding 0.0798g. FT-IR (4000–600 $cm^{-2}$): 3247.2 (br), 1562.73 (m), 1491.43 (w), 1417.59 (m), 1369.87 (w), 1345.83 (m), 1233.85 (m), 1222.91 (w), 1049.1 (w), 1019.47 (m), 1000.59 (s), 947.3 (w), 833.17 (w), 811.06 (m), 799.99 (m), 778.81 (w), 706.98 (m), 670.69 (vs), 681.12 (s), 636.35 (w), 622.93 (m)

**Synthesis of *mtn*-ZMOF:** $Cd(Ac)_2 \bullet H_2O$ (0.052g, 0.19575mmol), hexamethylenetetramine (0.050 g, 0.357mmol), water (0.25mL), DEF (1.125mL), $H_2O$ (0.25mL), sodium acetylacetonate (0.25mL, 0.174M in ethanol) tetrabutylammonium bromide (0.05mL, 1M in $H_2O$) were combined in a 20-mL vial, which was sealed and heated to105˚C for 23h and cooled to room temperature. Colorless polyhedral crystals were collected and air dried, yielding 0.0295g. FT-IR (4000–600 $cm^{-2}$): 3420.34 (br), 2968.2 (w), 2872.15 (w), 1660.03 (w), 1559.44 (m), 1418.31 (m), 1232.29 (m), 1111.4 (w), 1050.78 (w), 1001.01 (vs), 941.16 (w), 812.16 (m), 787.19 (w), 670.4 (s), 617.31 (s)

### 4.1.2 Results & Discussion

Reaction of cadmium acetate and HMTA in the presence of N,N'-diethylformamide and ethanol results in the formation of a mixture of *mep*-ZMOF and *sod*-ZMOF crystalline phases. Cadmium and diethylammonium cations are available for charge balance, and modification of such cation availability can direct the synthesis of different structures. Reaction of cadmium acetate and HMTA in an N,N'-dimethylacetamide/ethanol/water solution containing tetramethylammonium nitrate generates a pure crystalline phase of *sod*-ZMOF, in which cadmium and tetramethylammonium act to balance the charge of the framework. Additionally, reaction of cadmium acetate and HMTA in the presence of N,N'-diethylformamide, water, sodium acetylacetonate and tetrabutylammonium bromide produces a pure crystalline phase of *mtn*-ZMOF *via* the influence of sodium and tetrabutylammonium ions. This work demonstrates that, under specific conditions, varying SDAs can result in different ZMOFs built from HMTA-based TBUs connected through Cd-based linkers.

The *mep* topology, named for the natural silica-based mineral melanophlogite, is composed of pentagondodecahedral ($[5^{12}]$) and tetrakaidecahedral ($[5^{12}6^2]$) cages. The $[5^{12}6^2]$ cages, are fused though a common 6MR. The fusing 6MR and accompanying 12 5MRs constitute 12-ring double cups, 30 tetrahedral units, characteristic of the clathrasil family. In this anionic *mep*-ZMOF, HMTA coordinates to four Cd ions with N-Cd bond distances of 2.38-2.57 Å and N-Cd-N bond angles of 173.543-180.0°. It contains a $[5^{12}]$ cage with a van der Waals surface that allows the accomodation of a sphere with an approximate diameter of 8Å. The $[5^{12}]$ cage is built

from 20 HMTA nodes and 30 $Cd^{2+}$ linkers and has a -30 charge. The $[5^{12}6^2]$ cage is large enough to fit a sphere, within the van der Waals surface, approximately 8.4Å in diameter. This cage consists of 24 HMTA-based TBUs and 36 $Cd^{2+}$ linkers, each coordinated by 3 acetate anions, to yield a charge of -36. Cadmium linkers are

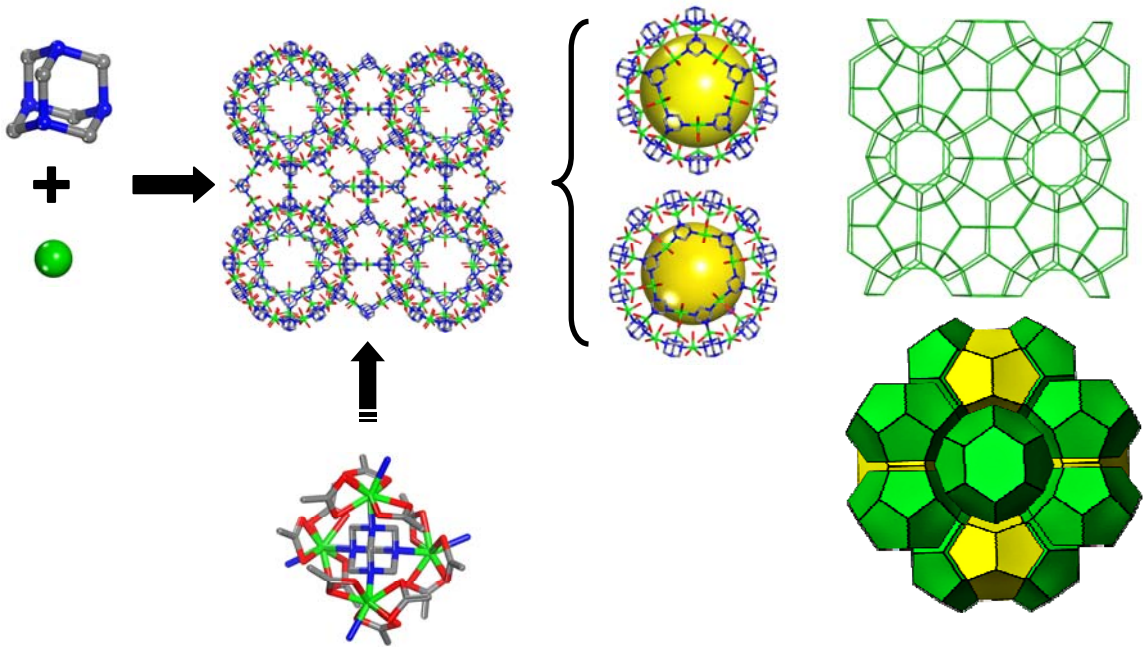

**Figure 4.9.** *mep*-ZMOF is constructed from $[5^{12}]$ (yellow) and $[5^{12}6^2]$ (green) cages.

coordinated by bidentate acetate ions, while, in some cases, one acetate ion exhibits monodentate coordination and the remaining oxygen atom assists to hold two cadmium ions within 5MRs. The distance from the centroid of one TBU to the next is approximately 8.1 Å, while the distance between tetrahedral atoms in the inorganic *mep* zeolite is approximately 3.1Å, demonstrating an expansion of approximately 2.6 times. The *mep* net has a transitivity of 3432, or 3,4,3, and 2 types of vertices, edges, faces, and tiles, respectively. The three types of vertices correspond to coordination sequences: $v_1$=4, 12, 26, 44, 64, 98, 144, 172, 222, 272; $v_2$=4, 12, 24, 42, 67, 95, 133,

177, 219, 277; $v_3$=4, 12, 25, 42, 69, 100, 129, 176, 229, 277.

The *mtn* net, also part of the clathrasil family, consists of $[5^{12}6^4]$ and $[5^{12}]$ tiles, with the 12-ring double cup arrangement. The *mtn* and *mep* nets both have transisitivties of 3432, three types of nodes, 4 kinds of edges, three faces, and two tiles. The three types of vertices correspond to the following coordination sequences: $v_1$=4, 12, 24, 36, 64, 112, 132, 156, 222, 264; $v_2$=4, 12, 24, 39, 66, 103, 130, 168, 216, 274; $v_3$=4, 12, 25, 43, 68, 95, 133, 177, 223, 274. The *mtn*-ZMOF is constructed from HMTA tetrahedral nodes and cadmium linkers, coordinated by three bidentate acetate ions, and each 5MR contains three sodium ions. The $[5^{12}6^4]$ cage is composed of 28 HMTA nodes and 24 Cd linkers. N-Cd bond distances are within the range of 2.36378 and 2.45615Å and N-Cd-N bond angles of 173.815-180.0°.

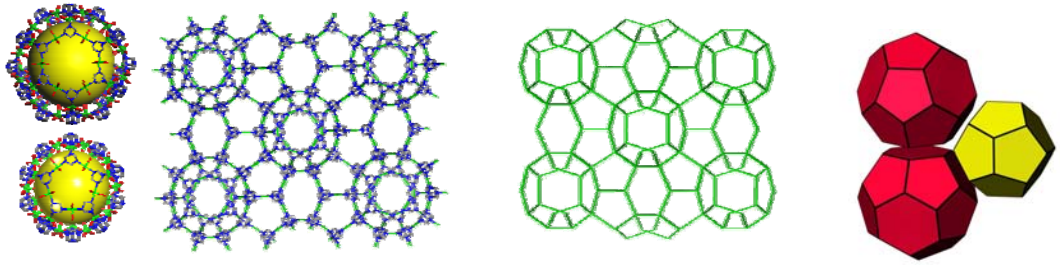

**Figure 4.10.** *mtn*-ZMOF a) ball and stick representation (guests and acetate ions are omitted for clarity), b) view of net, and c) $[5^{12}]$ (yellow) and $[5^{12}6^4]$ (red) tiles. d) Ball and stick representation of *sod*-ZMOF, e) view of net and f) packing of $[4^6.6^8]$ tiles.

The *sod*-ZMOF reported herein is constructred from HMTA linked through cadmium ions with N-Cd bond distances of 2.43540Å and N-Cd-N bond angles of 160.202˚. The distance between the centroid of one TBU to the next is 7.738Å, while the tetrahedral nodes in the aluminosilicate zeolite are about 3.143Å apart, thus this *sod*-ZMOF is over twice as large as the purely inorganic analogue. The framework consists of β-cages with adequate space to encapsulate a sphere of ~10Å in diameter. Each β-cage is constructed from 24 HMTA nodes and 36 cadmium

linkers, resulting in a -36 charge that is balanced by $Cd^{2+}$ ions in the 4MR windows and six tetramethylammonium ions in each cage. As in *mep*-ZMOF, acetate ions exhibit bidentate coordinate to the cadmium linkers, while some display monodentate coordination and the remaining oxygen atom assists in stabilizing $Cd^{2+}$ ion guests.

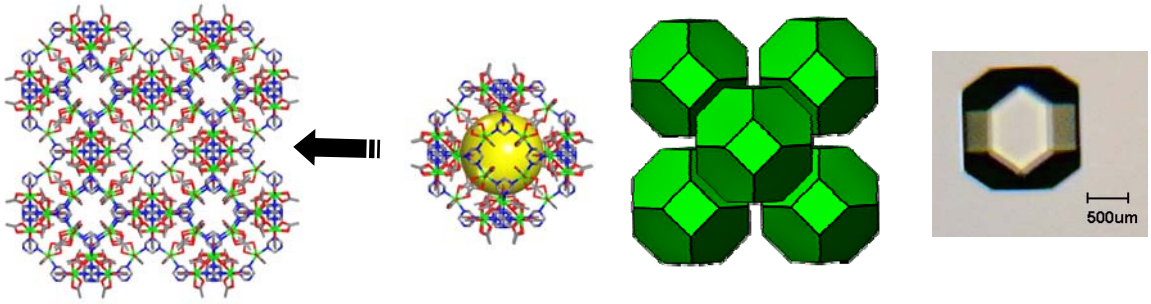


**Figure 4.11.** *sod*-ZMOF, constructed from cadmium and HMTA.

This work demonstrates that cadmium ions can be coordinated by three acetate ions and two axial nitrogen atoms to link HMTA-based TBUs, resulting in anionic ZMOFs. Various zeolite-*like* topologies can be accessed by altering the types of cations that are present as SDAs in these metal-organic materials.

## 4.4 Conclusions

Various organic ligands and single-metal ions can be used for the design of ZMOFs, however knowledge and access to appropriate synthetic conditions is limited. Three approaches utilizing (1) metal-organic cube-based SBBs, (2) single-metal ion-based $MN_2(CO_2)_4$ MBBs, and (3) organic TBUs represent advancements in the design and synthesis of ZMOFs. Experimentation with appropriate metal-organic monomers resulted in intentional formation of building blocks and, ultimately, established reaction conditions for numerous zeolite-like networks.

## Chapter 5: Conclusions and Future Outlook

As approaches for MOM design converge with building block ideals, the ability to ultimately impose utilitarian design becomes feasible for construction of materials for intended functions. The research presented in this thesis is primarily concerned with advancing strategies for the construction of pre-designed metal-organic materials, and in summary, the following notions have been demonstrated.

Single-metal ion-based molecular building blocks, $MN_x(CO_2)_y$, can indeed be successfully employed in the rational construction of 0-, 1-, 2-, and 3-dimensional MOMs. N-,O-Heterochelating ligands can unify aspects of nitrogen based ligands and carboxylate based ligands to induce rigidity and directionality. Differences in orientations of chelation and coordination in MBBs, which can be influenced by reaction conditions, have structure directing effects on networks. The metal sources and/or ligands in MBBs can be changed to create isoreticular nets. $MN_2O_2$ tetrahedral BUs can be derived from $MN_2(CO_2)_4$ MBBs and employed in the synthesis of ZMOFs, which are highly valuable targets. Additionally, metal-organic cubes, assembled from $MN_3(CO_2)_3$ MBBs, can be used as SBBs in the construction of ZMOFs. Suitable zeolite targets in metal-organic crystal chemistry, for such SBBs, can be revealed by relationships with augmented edge transitive 8-connected nets.

In addition, a rare coordination of cadmium has been accessed by coordination of organic-based tetrahedral nodes to create $MN_4(CO_2)_3$ based MBBs for the directed

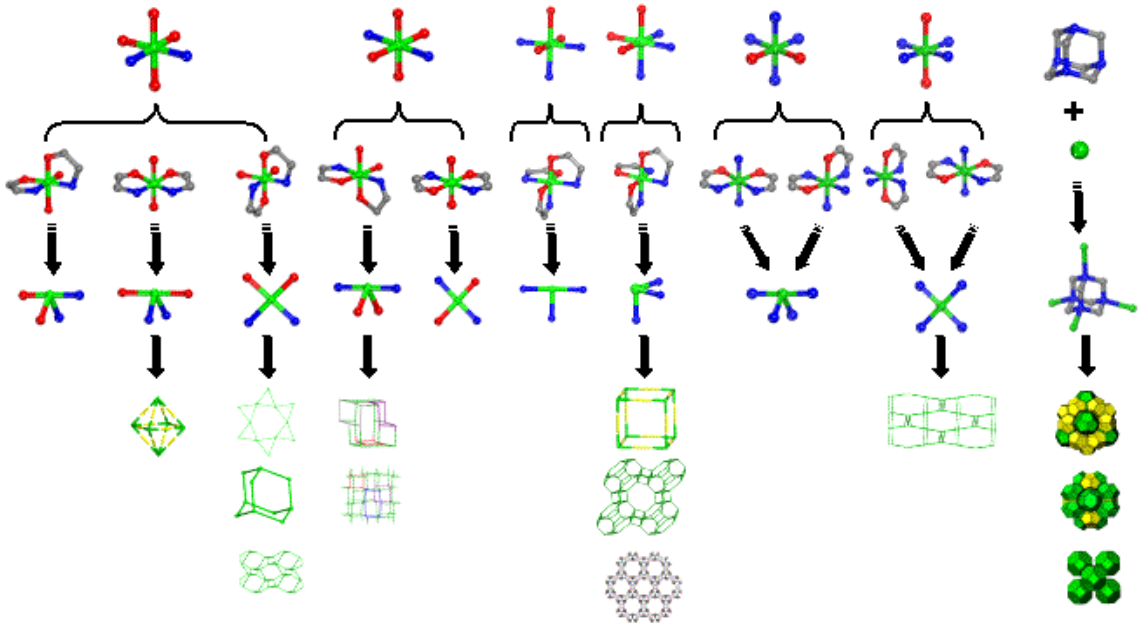

**Figure 5.1.** Summary of structured from $MN_x(CO_2)_y$ Molecular Building Blocks.

synthesis of ZMOFs. Anionic auxiliary ligands, specifically acetate, can be exploited for the synthesis of charged networks, and ultimately charge-balancing structure directing agents can be used to access various ZMOFs.

This work demonstrates that highly valuable target nets can be reconstructed with metal-organic MBBs on expanded scales, crystallized as pure phases, and employed in ion-exchange applications. Ion-exchange capabilities manifest opportunities to tune properties of crystalline materials for specific applications. As construction of designed materials is advanced, with approaches based on building blocks, materials with tunable cavities and channel sizes can be obtained. Ideally reaction conditions can be established and used in future syntheses of specifically intended building blocks. Additionally, linker angularity can be adjusted to compensate for the geometrical attributes of commonly formed BUs. Such MOMs can be used as platforms for innumerable guests, resulting in materials with tunable properties.

With the continuation of developments in design and synthesis correlations, MOMs offer a means to tailor-make functional solid state materials for specific applications. Such materials are highly beneficial to areas including, but not limited to, transportation, environmental technologies, space exploration, microelectronics, catalysis, chiral separations, and biomedical and pharmaceutical applications. As aspects of design mature, correlations between specific MOMs and desired applications are becoming stronger.

## References


1 Rowsell, J.L.C., Yaghi, O.M., *Microporous Mesoporous Mater.* **2004,** *73*, 3.

2. Barrett, C.S., *Structure of Metals, 2nd ed.*, McGraw-Hill, New York, **1952**,1.

3. Stein, A., Keller, S.W., Mallouk, T.E. *Science*, **1993,** *259*, 3101, 1558.

4. Kitigawa, S., Kitaura, R., Noro, S. *Angew. Chem. Int. Ed.* **2004**, *43,* 2334.

5. Griffith, R. L. *J. Chem. Phys.* **1943**, *11*, 499.

6. (a) Munakata, M., Kurodasowa, T., Maekawa, M., Honda, A., Kitagawa, S. *J. Chem. Soc., Dalton Trans.* **1994,** *19,* 2771. (b)Yaghi, O.M., Li, H. *J. Am. Chem. Soc.* **1995**, *117,* 10401.

7. Fujita, M., Kwon, Y. J., Washizu S., Ogura, K. *J. Am. Chem. Soc.* **1994** *116,* 1151.

8. Kinoshita,Y., Matsubara, I., Higushi, T., Saito,Y. *Bull. Chem. Soc. Jpn.*, **1959**, *32*, 1221.

9. Hoskins, B.F., Robson, R. *J. Am. Chem. Soc.* **1989**, *111*, 5962.

10. (a) Carlucci., L., Ciani, G., Proserpio, D.M., Rizzato, S. *Chem. Commun*. **2001**, 1198-1199. (b) Halder, G. J., Kepert, C. J., Moubaraki, B., Murray, K. S., Cashion, J. D. *Science,* **2002,** *298,* 1762. (c) Iwamoto T.. The Hofmann-type and related inclusion compounds. In: Atwood JL, Davies JED, MacNicol, DD, editors. Inclusion Compounds: Structural Aspects of Inclusion Compounds Formed by Inorganic and Organometallic Host Lattices. **1984** London: Academic Press. p 29.

11. Kondo,M., Yoshitomi, T., Matsuzaka, H., Kitagawa, S., Seki, K. *Angew. Chem. Int. Ed. Engl.* **1997** *36*, 16, 1725.

12. Kondo, M., Shimamura, M., Noro, S., Minakoshi, S., Asami, A., Seki, K., Kitagawa, S. *Chem. Mater.* **2000**, *12*, 1288.

13. Hoskins, B.F., Robson, R. *J. Am. Chem. Soc.* **1990**, *112*, 1546.

14. O.M. Yaghi, H. Li, *J. Am. Chem.* Soc, **1996**, *118*, 295.

15. Lopez, S., Kahraman, M., Harmata, M., Keller, S.W. *Inorg. Chem.* **1997**, *36*, 6138.

16. Carlucci, L., Ciani, G., Proserpio, D.M., Sironi, A. *Chem. Commun*. **1994,** 2755.

17. MacGillivray, L.R., Subramanian, S., Zaworotko, M.J. *Chem. Commun.* **1994**, 1325.

18. Hirsch, K.A., Venkataraman, D., Wilson, S.R., Moore, J.S., Lee, S. *Chem. Commun.* **1995**, *21,* 2199.

19. Hirsch, K.A., Wilson, S.R., Moore, J.S. *Inorg. Chem.* **1997**, *36*, 2960.

20. Sinzger, K., Hünig, S., Jopp, M., Bauer, D., Bietsch, W., von Schütz, J.U., Wolf, H.C., Kremer, R.K., Metzenthin, T., Bau, R., Khan, S.I., Lindbaum, A., Lengauer, C.L., Tilmanns, E. *J. Am. Chem. Soc.* **1993**, *115*, 7696.

21. Cromer, D.T., Larson, A.C. *Acta Cryst*. **1972**, *B28*, 1052.

22. Zaworotko, M. J. *Chem. Soc. Rev.* **1994**, 283.

23. Yaghi, O.M., O'Keeffe, M., Ockwig, N.W., Chae, H.K., Eddaoudi, M., Kim, J. *Nature* **2003**, *423,* 705.

24. Yaghi, O.M., Li H., Davis, C., Richardson, D., Groy, T. L. *Acc. Chem. Res.* **1998**, *31,* 474.

25. Li, H., Eddaoudi, M., O'Keeffe, M., Yaghi, O. M. *Nature* **1999.** *402*, 276.

26. Li, H., Eddaoudi, M., Groy, T.L., Yaghi, O. M. *J. Am. Chem. Soc.* **1998.** *120,* 8571.

27. Chui, S.S.-Y., Lo, S.M.-F., Charmant, J. P. H., Orpen, A. G., Williams, I. D. *Science* **1999,** *283,* 1148.

28. Eddaoudi, M., Moler, D. B., Li, H., Chen, B., Reineke, T. M., O'Keeffe, M., Yaghi, O. M. *Acc. Chem. Res.* **2001**, *34,* 319.

29. Yaghi, O.M., Li, G., Li, H. *Nature*, **1995,** *378*, 6558, 703.

30. van Niekerk, J.N., Schoening, F.R.L. Schoening, *Acta Cryst.* **1953**, *6*, 227.

31. Eddaoudi, M., Kim, J. Wachter, J.B., Chae, H.K., O'Keeffe, M., Yaghi, O.M., *J. Am. Chem. Soc.,* **2001**, 123, 4368.

32. Chen, B., Eddaoudi, M., Hyde, S.T., O'Keeffe, Yaghi, O.M. *Science*, **2001** *291*, 1021.

33. Bourne, S.A., Lu, J., Mondal, A., Moulton, B., Zaworotko, M.J. *Angew. Chem., Int. Ed.* **2001**, *40*, 2111.

34. Kim, J., Chen, B., Reineke, T.M., Li. H., Eddaoudi, M., Moler, D., O'Keeffe, M., Yaghi., O.M., *J. Am. Chem. Soc.* **2001,** 123, 8239.

35. Eddaoudi, M., Li, H., Yaghi, O.M. *J. Am. Chem. Soc.* **2000**, *122*, 1391.

36. Eddaoudi, M., Kim, J., Rosi, N., Vodak, D., Wachter, J., O'Keeffe, M., Yaghi, O.M. *Science*, **2002,** *295*, 469.

37. O'Keeffe, M., Hyde, B. G. *Crystal Structures I: Patterns and Symmetry* **1996,** Mineralogy Society of America, Washington D.C.Rosi, N.L., Eckert, J.,

38. Jiang, C., Yu, Z., Wang, S., Jiao, C., Li, J., Wang, Z., Cui, Y. *Eur. J. Inorg. Chem.* **2004***, 18I, 366.*

39. Batten, S.R., Murray, K.S. *Coor. Chem. Rev.* **2003***, 246 (1-2),* 103.

40. Murugavel, R., Anantharaman, G., Krishnamurthy, D., Sathiyendiran, M., Walawalkar, M.G. *Proceedings of the Indian Academy of Sciences-Chemical Sciences* **2000***, 112,* 3, 273.

41. Wan, S., Huang, Y., Li, Y., Sun, W. *Microporous Mesoporous Mater.* **2004,** *73*, 101.

42. Yang, G., Raptis, R.G. *Chem. Commun.* **2004**, 2058.

43. Zhao, W., Fan, J., Okamura, T., Sun, W.Y., Ueyama, N. *New J. Chem.* **2004***, 28*, 9, 1142.

44. Liu, H., Yu, S., Huang, H., Zhang, Z. *Aust J. Chem*. **2003**, *56*, 671.

45. Lu, J.Y., Babb, A.M.*, Inorg. Chem. Commun* **2001,** *4,* 716.

46. Batten, S. R.; Robson, R. *Angew. Chem., Int. Ed.* **1998**, *37*, 1461.

47. Robson, R. *J. Chem. Soc., Dalton Trans.* **2000**, 3735.

48. Brunner, G.O., Laves, F. *Wiss. Z. Techn. Univers. Dresden* **1971,** *20,* 387.

49. Baerlocher, Ch., Meier, W. M., Olson, D. H. *Atlas of Zeolite Framework Types: Fifth Revised Edition* **2001** Elsevier, Published on behalf of the Structure Commission of the International Zeolite Association

50. O'Keeffe, M.; Yaghi, O. M. *Reticular Chemistry Structure Resource*: http://okeeffe-ws1.la.asu.edu/RCSR/home.htm.

51. Banerjee, R., Phan, A., Wang, B., Knobler, C., Furukawa, H., O'Keeffe, M., Yaghi, O.M. *Science* **2008**, *319,* 939.

52. Férey, G., Mellot-Draznieks, C., Serre, C., Milange, F., Dutour, J., Surblé, S., Margiolaki, I. *Science* **2005**, *309,* 2040.

53. Park, Y. K., Choi, S. B., Kim, H., Kim, K., W, B.-H., Choi, K., Choi, J.-S., Ahn, W.-S., Won, N., Kim, S., Jung, D. H., Choi, S.-H., Kim, G.-H., Cha, S.-S., Jhon, Y. H., Yang, J. K., Kim, J. *Angew. Chem. Int. Ed.* **2007***, 46,* 8230.

54. Cheetham, A.K., Rao, C. N. R., Feller, Russell K. *Chem. Commun.* **2006**, *46*, 4780.

55. Seo, J.S., Whang, D., Lee, H., Jun, S. I., Oh, J., Jeon, Y. J., Kim, K. *Nature* **2000,** *404,* 982.

56. Maurizot, V., Yoshizawa, M., Kawano, M., Fujita, M. *Dalt. Trans.* **2006**, 2750.

57. Busca, G. *Chem. Rev.* **2007**, *107,* 11, *5366.*

58. Kaye, S.; Dailly, A.; Yaghi, O.M.; Long, J.R. J. Am. Chem. Soc. 2007, 129, 14176.

59. Kitagawa, S.; Kondo, M. Angew. Chem., Int. Ed. Engl. **1997**, 36, 1725.

60. Ozin, G. A. *Chem. Commun.* **2000**, 419.

61. Friedrichs, O. D., O'Keeffe, M., Yaghi, O. M. *Acta Cryst.* **2003***, A59,* 22.

62. Friedrichs, O. D., O'Keeffe, M., Yaghi, O. M. *Acta Cryst.* **2003***, A59*, 515.

63. Friedrichs, O. D., O'Keeffe, M., Yaghi, O. M. *Acta Cryst.* **2006***, A62*, 350.

64. Friedrichs, O. D., O'Keeffe, M., Yaghi, O. M. *Acta Cryst.* **2007***, A63*, 344.

65. Liu, Y., Kravtsov, V. Ch., Larsen, R., Eddaoudi, M. *Chem. Commun.* **2006**, 1488.

66. Ciurtin, D. M., Smith, M. D., zur Loye, H.-C., *Datlon Trans.* **2003,** 1245.

67. Liu, Y., Kravtsov, V., Beauchamp, D. A., Eubank, J. F., Eddaoudi, M. *J. Am. Chem. Soc.* **2005**, *127,* 7266.

68. Brant, J. A., Liu, Y., Sava, D. F., Beauchamp, D., Eddaoudi, M. *J. Mol. Struct.* **2006,** *796,* 160.

69. Kiani, S., Tapper, A., Staples, R. J., Stavropoulos, P. *J. Am. Chem. Soc.* **2000,** *122,* 7503.

70. Basu, S., Peng, S., Lee, G., Bhattacharya, S. *Polyhedron* **2005**, *24,* 157.

71. Fu, A., Wang, D. *Acta Crystallogr., Sect. E: Struct. Rep.* **2005**, m481.

72. Shi, Z., Feng, S., Sun, Y., Hua, J. *Inorg. Chem.* **2001,** *40,* 5312.

73. Liu, Y., Kravtsov, V., Walsh, R. D., Poddar, P., Srikanth, H., Eddaoudi, M. *Chem. Commun.* **2004,** 2806.

74. Saint Plus, v. 6.01, Bruker Analytical X-ray, Madison, WI, 1999.

75. Sheldrick, G. M. SHELXTL, v. 5.10; Bruker Analytical X-ray, Madison, WI, 1997.

76. Dolomanov, O. V., Blake, A. J., Champness, N. R., Schröder *J. Appl. Cryst.* **2003**, *36,* 1283.

77. Blatov, V. A., Carlucci, L., Ciani, G., Prosperpio, D. M. *CrystEngComm* **2004**, *6,* 377.

78. Spek, A. L. *J. Appl. Cryst.* **2003**, *36*, 7.

79. Delgado-Friedrichs, O. *The Gavrog Project:* http://gavrog.sourceforge.net/

80. Smith, J.V. *Chem. Rev.* **1988**, *88*, 149.

81. Baerlocher, C. McCusker, L.B.*Database of Zeolite Structures:* http://www.iza-structure.org/databases/

82. Davis, M.E. *Nature* **2002,** *417*, 813.

83. Babel, S., Kurniawan, T. A. *J. Hazardous Materials* **2003**, *97,* 219.

84. Gould, R.F. *Molecular Sieve Zeolites-I.* **1971**, A.C.S.: Washington, D.C.

85. Gould, R.F. *Molecular Sieve Zeolites-II* **1971,** A.C.S.: Washington, D.C.

86. Li, C.P., Wong, N.B., Lee, C.S., Lee, S.T., Teo, B.K. *Chemical Physics Letters* **2004,** 365, 22.

87. Pansini, M. *Mineralium Deposita* **1996**, *31,* 6, 563.

.

88. Moulton, B.; Lu, J.; Mondal, A. and Zaworotko, M. *Chem. Commun.* **2001**, 863.

89. Cairns, A. J.; Perman, J. A.; Wojtas, L.; Kravtsov, V. Ch.; Alkordi, M. H.; Eddaoudi, M.; Zaworotko, M. J. *J. Am. Chem. Soc.* **2008**, *130,* 5, 1560.

90. Nouar, F.; Eubank, J. F; Bousquet, T; Wojtas, L; Zaworotko, M. J.; Eddaoudi, M. *J. Am. Chem. Soc.* **2008**, *130,* 6, 1833.

91. O'Keeffe, M.; Eddaoudi, M.; Li, H.; Reineke, T.; Yaghi, O. M. *J. Solid State Chem.,* **2000**, *152*, 3.

92. Sava, D. F., Kravtsov, V. Ch., Nouar, F., Wojtas, L., Eubank, J. F., Eddaoudi, M. *J. Am. Chem. Soc.* **2008**, *130,* 12, 3768.

93. Fang, Q., Zhu, G., Xue, M., Sun, J., Wei, Y., Qui, S., Xu, R. *Angew. Chem. Int. Ed.* **2005**, 44, 3845.

# Appendices

## Appendix I: Crystallography Tables

| **Compound** | **ME086** | **ME089** | **ME096** |
|---|---|---|---|
| **Chemical Formula** | $Cd(C_4N_2O_2H_3)_2$ | $Cd_2(C_5N_2O_4H)_2$ $(C_2N_2H_4)_{2.5}$ $C_3NOH_7$ | $Cd_2(C_4N_2O_2H_3)_2$ $(H_2O)_2(C_3NOH_7)_2$ |
| **Formula Weight** | 334.58 | 768.26 | 867.38 |
| **Temperature, K** | 100 | 100 | 100 |
| **Crystal System** | Orthorhombic | Monoclinic | Monoclinic |
| **Space Group** | Fdd2 | P21/n | C2/c |
| **a, Å** | 11.2859(18) | 11.5625(8) | 24.483(5) |
| **b, Å** | 19.388(3) | 15.0527(10) | 10.929(2) |
| **c, Å** | 8.3726(14) | 17.0502(11) | 12.810(3) |
| **α, deg** | 90 | 90 | 90 |
| **β, deg** | 90 | 95.9080(10) | 113.619(4) |
| **γ, deg** | 90 | 90 | 90 |
| **V, Å$^3$** | 1832.0(5) | 2951.8(3) | 3140.5(11) |
| **Z** | 8 | 4 | 4 |
| **ρ, g·cm$^{-3}$** | 2.426 | 1.729 | 1.834 |
| **μ, mm$^{-1}$** | 2.395 | 1.504 | 1.433 |
| **F(000)** | 1296 | 1504 | 1728 |
| **Crystal Size, mm** | 0.09 x 0.11 x 0.12 | 0.1x0.1x0.1 | 0.1x0.1x0.1 |
| **θ range for data collection, deg** | 3.2 to 24.9 | 2.2 to 28.4 | 3.2 to 28.3 |
| **Limiting indices** | -7<=h<=13<br>-22<=k<=22<br>-9<=l<= 9 | -14<=h<=15<br>-19<=k<=16<br>-22<=l<= 15 | -20<=h<=30<br>-12<=k<=14<br>-16<=l<= 13 |
| **Reflections collected** | 1788 | 18457 | 7391 |
| **Unique Reflections** | 775 | 6833 | 3454 |
| **R(int)** | 0.033 | 0.06 | 0.056 |
| **Goodness-of-fit on F$^2$** | 1.06 | 1.04 | 1.01 |
| **Final R indices** | R1=0.0213, wR2=0.0499 | R1=0.0603, wR2=0.1525 | R1=0.0522, wR2=0.1105 |
| **Max. and Min. Resd. Dens., e·Å$^{-3}$** | 0.36 and -0.39 | 2.55 and -1.17 | 1.43 and -1.22 |

**Appendix I (continued)**

| Compound | ME184 | ME207 | ME299 |
|---|---|---|---|
| **Chemical Formula** | $Cd(C_6N_2O_2H_7)_2$ | $(Cd(C_7O_4NH_3)_2)_3$ | $Cd_{12}(C_5N_2O_4)_{18}$ |
| **Formula Weight** | 390.6 | 1327.9 | 4086.1 |
| **Temperature, K** | 298 | 100 | 298 |
| **Crystal System** | Orthorhombic | Trigonal | Trigonal |
| **Space Group** | P212121 | R-3c | R-3 |
| **a, Å** | 11.549(4) | 16.178(3) | 17.1507 |
| **b, Å** | 11.666(3) | 16.178(3) | 17.1507 |
| **c, Å** | 11.762(4) | 52.30(2) | 42.0808 |
| **α, deg** | 90 | 90 | 90 |
| **β, deg** | 90 | 90 | 90 |
| **γ, deg** | 90 | 120 | 120 |
| **V, Å$^3$** | 1584.7(9) | 11855(5) | 10719.59 |
| **Z** | 4 | 6 | 2 |
| **ρ, g·cm$^{-3}$** | 1.638 | 1.501 | 1.379 |
| **μ, mm$^{-1}$** | 1.397 | 0.879 | 1.248 |
| **F(000)** | 776 | 5261 | 4254 |
| **Crystal Size, mm** | 0.07x0.08x0.1 | 0.1x0.1x0.02 | 0.1x0.1x0.1 |
| **θ range for data collection, deg** | 2.5 to 25.1 | 1.6 to 22.0 | |
| **Limiting indices** | -13<=h<=12<br>-12<=k<=12<br>-14<=l<= 10 | -16<=h<=16<br>-16<=k<=17<br>-55<=l<= 34 | |
| **Reflections collected** | 6550 | 12031 | |
| **Unique Reflections** | 2704 | 1621 | |
| **R(int)** | 0.106 | 0.166 | |
| **Goodness-of-fit on F$^2$** | 0.84 | 1.02 | |
| **Final R indices** | R1=0.0558,<br>wR2=0.1193 | R1=0.0577,<br>wR2=0.1107 | |
| **Max. and Min. Resd. Dens., e·Å$^{-3}$** | 0.6 and -0.59 | 0.52 and -0.44 | |

**Appendix I (continued)**

| **Compound** | **ME511** | **ME694** |
|---|---|---|
| **Chemical Formula** | $Cd(C_5N_2O_4H_2)(C_2N_2H_4)$ | $In_3(C_7O_4NH_3)_6$ $(C_4N_2H_{12})O_{12}$ |
| **Formula Weight** | 325.58 | 1664.12 |
| **Temperature, K** | 100(2) | 293(2) |
| **Crystal System** | Tetragonal | Hexagonal |
| **Space Group** | I41/acd | R-3c |
| **a, Å** | 12.5699(12) | 26.64(3) |
| **b, Å** | 12.5699(12) | 26.64(3) |
| **c, Å** | 26.676(5) | 40.83(6) |
| **α, deg** | 90 | 90 |
| **β, deg** | 90 | 90 |
| **γ, deg** | 90 | 120 |
| **V, Å$^3$** | 4214.9(9) | 25094(52) |
| **Z** | 16 | 12 |
| **ρ, g·cm$^{-3}$** | 2.052 | 1.321 |
| **μ, mm$^{-1}$** | 2.078 | 0.9 |
| **F(000)** | 2544 | 9893 |
| **Crystal Size, mm** | 0.15x0.1x0.1 | 0.10 x 0.10 x 0.10 |
| **θ range for data collection, deg** | 1.8 to 25.2 | 2.14 to 15.86 |
| **Limiting indices** | -15<=h<=7<br>-15<=k<=15<br>-32<=l<=31 | -11<=h<=20<br>-20<=k<=1<br>-31<=l<=12 |
| **Reflections collected** | 9724 | 3269 |
| **Unique Reflections** | 968 | 1316 |
| **R(int)** | 0.023 | 0.1538 |
| **Goodness-of-fit on F$^2$** | 1.494 | 1.148 |
| **Final R indices** | R1 = 0.0596,<br>wR2 = 0.1436 | R1 = 0.1283,<br>wR2 = 0.3284 |
| **Max. and Min. Resd. Dens., e·Å$^{-3}$** | 0.970 and -1.164 | 0.872 and -0.726 |

**Appendix I (continued)**

| **Compound** | **JB9545** | **ME688** |
|---|---|---|
| **Chemical Formula** | $Cd_{0.75}(C_5N_2O_4H)(C_3NOH_7)_{0.75}$ | $Cd_{0.6}(C_5N_2O_4H)(C_4N_2)$ |
| **Formula Weight** | 300.4 | 298.71 |
| **Temperature, K** | 100 | 100 |
| **Crystal System** | Monoclinic | Trigonal |
| **Space Group** | P21/c | R-3m |
| **a, Å** | 14.725(6) | 37.907(18) |
| **b, Å** | 14.664(5) | 37.907(18) |
| **c, Å** | 23.550(9) | 31.72 |
| **α, deg** | 90 | 90 |
| **β, deg** | 106.678(6) | 90 |
| **γ, deg** | 90 | 120 |
| **V, Å$^3$** | 4871(3) | 39473(36) |
| **Z** | 16 | 90 |
| **ρ, g·cm$^{-3}$** | 1.639 | 1.131 |
| **μ, mm$^{-1}$** | 1.379 | 0.780 |
| **F(000)** | 2348 | 13038 |
| **Crystal Size, mm** | 0.09x0.12x0.15 | 0.06x0.06x0.06 |
| **θ range for data collection, deg** | 1.8 to 25.14 | 2.21 to 21.5 |
| **Limiting indices** | -17 to 17<br>-9 to 17<br>-27 to 26 | -20 to 37<br>-38 to 38<br>-24 to 32 |
| **Reflections collected** | 24232 | 23271 |
| **Unique Reflections** | 8611 | 5329 |
| **R(int)** | 0.15 | 0.175 |
| **Goodness-of-fit on F$^2$** | S=1.011 | S=1.102 |
| **Final R indices** | R1=0.1100, wR2=0.2659 | R1=0.1310, wR2=0.3159 |
| **Max. and Min. Resd. Dens., e·Å$^{-3}$** | 1.642 and -1.145 | 1.141 and -1.658 |

**Appendix I (continued)**

| **Compound** | ***ana*-ZMOF (ME654)** | ***sod*-ZMOF(2) (ME658)** |
|---|---|---|
| **Chemical Formula** | $In_{0.5}(C_7NO_4H_3)$ | $In_{0.5}(C_7NO_4H_3)(C)(O)$ |
| **Formula Weight** | 327.68 | 262.14 |
| **Temperature, K** | 187 | 293(2) |
| **Crystal System** | Cubic | Hexagonal |
| **Space Group** | Ia-3d | R-3 |
| **a, Å** | 37.469(16) | 35.305(5) |
| **b, Å** | 37.469(16) | 35.305(5) |
| **c, Å** | 37.469(16) | 35.305(5) |
| **α, deg** | 90 | 90 |
| **β, deg** | 90 | 90 |
| **γ, deg** | 90 | 120 |
| **V, Å$^3$** | 52604(39) | 17300 |
| **Z** | 96 | 36 |
| **ρ, g·cm$^{-3}$** | 0.978 | 0.906 |
| **μ, mm$^{-1}$** | 0.577 | 0.647 |
| **F(000)** | 15462 | 4619 |
| **Crystal Size, mm** | 0.1x0.1x0.1 | 0.1x0.1x0.1 |
| **θ range for data collection, deg** | 1.53 to 17.08 | 1.99 to 20.82 |
| **Limiting indices** | -18 to 21<br>-7 to 32<br>-13 to 32 | -75 to 35<br>-35 to 32<br>-15 to 15 |
| **Reflections collected** | 9218 | 19560 |
| **Unique Reflections** | 1324 | 4021 |
| **R(int)** | 0.1391 | 0.1043 |
| **Goodness-of-fit on F$^2$** | 1.240 | 1.161 |
| **Final R indices** | R1=0.1186,<br>wR2=0.3150 | R1=0.1415,<br>wR2=0.3438 |
| **Max. and Min. Resd. Dens., e·Å$^{-3}$** | 0.483 and -0.538 | 1.049 and -1.124 |

**Appendix I (continued)**

| Compound | *mep*-ZMOF (ME474) | *sod*-ZMOF (ME312) | *lta*-ZMOF (ME500) |
|---|---|---|---|
| **Chemical Formula** | $CdC_{4.14}N_4O_{0.53}H_8$ | $Cd_{2.50}\ C_{21.04}\ N_5\ O_{17.19}\ H_{43.084}$ | $Cd_4(C_5O_4N_2H_2)_4\ (C_5O_4N_2H)(C_4N_2H_{12})_{0.5}\ Na_4(C_2H_5OH)_{1.25}\ (H_2O)_{9.25}$ |
| **Formula Weight** | 234.52 | 917.77 | 943.69 |
| **Temperature, K** | 163(2) | 100(2) | 100(2) |
| **Crystal System** | Cubic | Cubic | Trigonal |
| **Space Group** | Pm-3n | Im-3m | R-3m |
| **a, Å** | 34.0147 | 21.8867(14) | 40.637(5) |
| **b, Å** | 34.0147 | 21.8867(14) | 40.637(5) |
| **c, Å** | 34.0147 | 21.8867(14) | 39.063(7) |
| **α, deg** | 90 | 90 | 90 |
| **β, deg** | 90 | 90 | 90 |
| **γ, deg** | 90 | 90 | 120 |
| **V, Å$^3$** | 39355.01 | 10484.3(12) | 55865(13) |
| **Z** | 188 | 12 | 36 |
| **ρ, g·cm$^{-3}$** | 1.860 | 1.744 | 1.01 |
| **μ, mm$^{-1}$** | 2.545 | 1.588 | 0.751 |
| **F(000)** | 21242 | 5491 | 16561 |
| **Crystal Size, mm** | 0.10 x 0.10 x 0.10 | 0.10 x 0.10 x 0.10 | 0.10 x 0.10 x 0.10 |
| **θ range for data collection, deg** | 2.54 to 19.19 | 2.28 to 23.23 | 1.74 to 20.05 |
| **Limiting indices** | -29<=h<=28, -11<=k<=31, -29<=l<=31 | -23<=h<=24 -18<=k<=24 -24<=l<=16 | -39<=h<=36 -37<=k<=37 -11<=l<=37 |
| **Reflections collected** | 46794 | 19464 | 27467 |
| **Unique Reflections** | 2681 | 776 | 5997 |
| **R(int)** | 0.1163 | 0.0658 | 0.0955 |
| **Goodness-of-fit on F$^2$** | 0.963 | 1.101 | S=1.01 |
| **Final R indices** | R1=0.1334, wR2=0.2845 | R1=0.0501, wR2 = 0.1439 | R1 = 0.0973, wR2 = 0.2266 |
| **Max. and Min. Resd. Dens., e·Å$^{-3}$** | 0.956 and -0.946 | 0.602 and -0.758 | 0.643 and -0.607 |

## Appendix II: Thermal Gravimetric Analysis

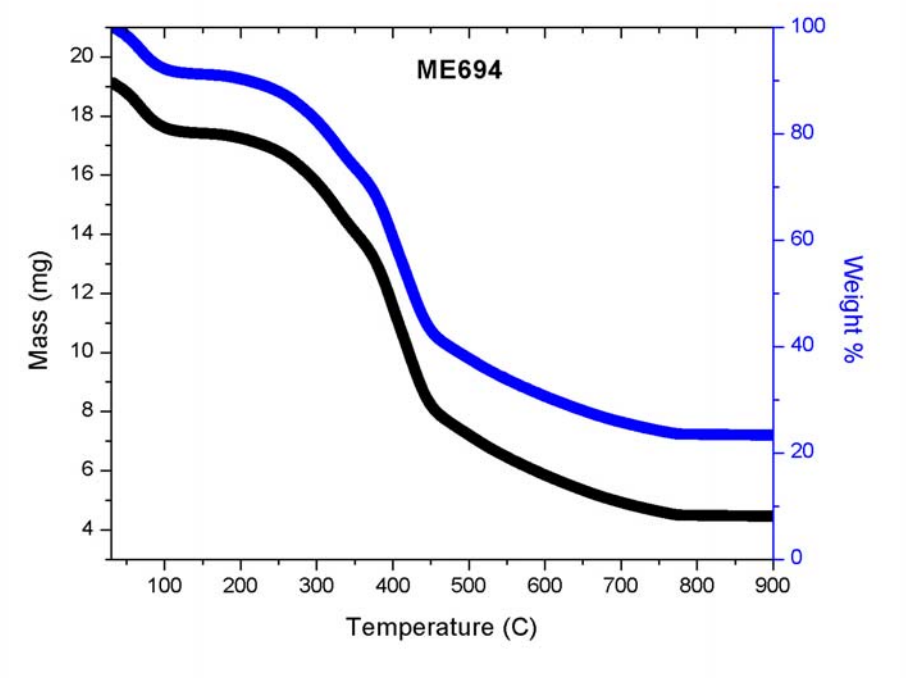


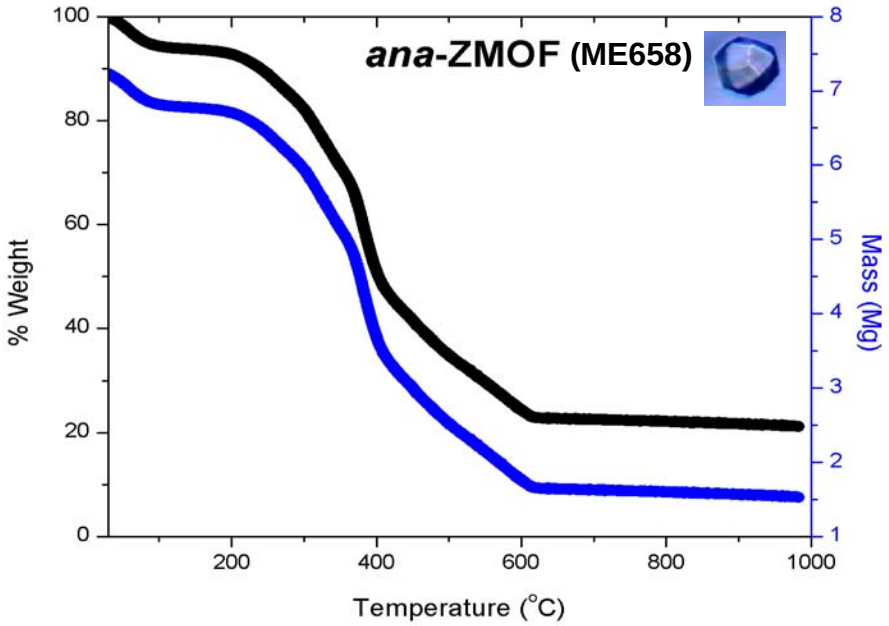

**Appendix II (continued)**

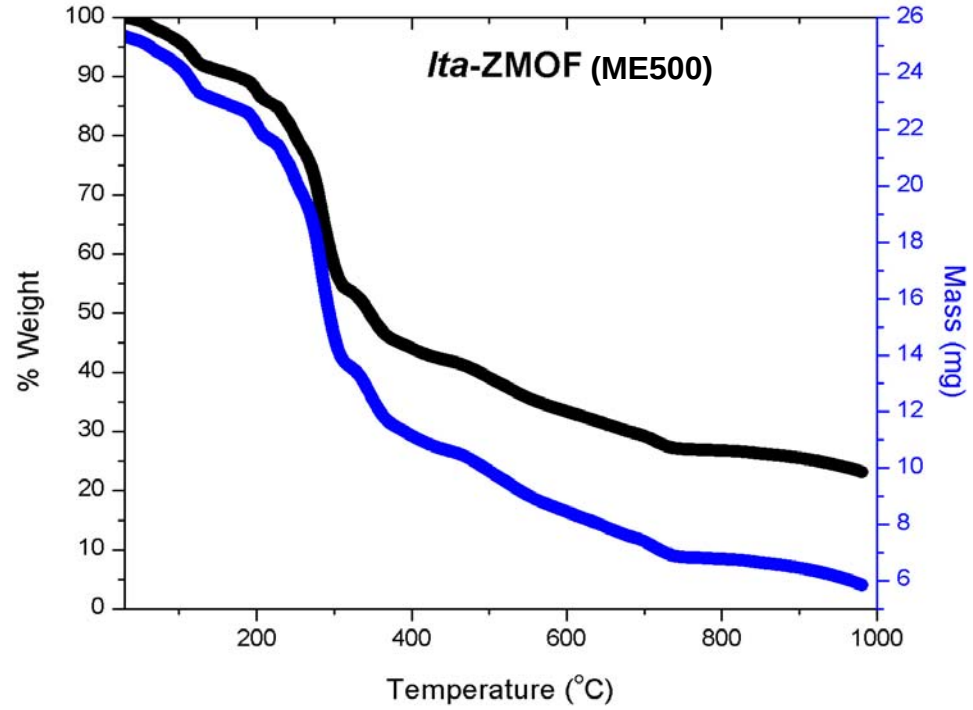


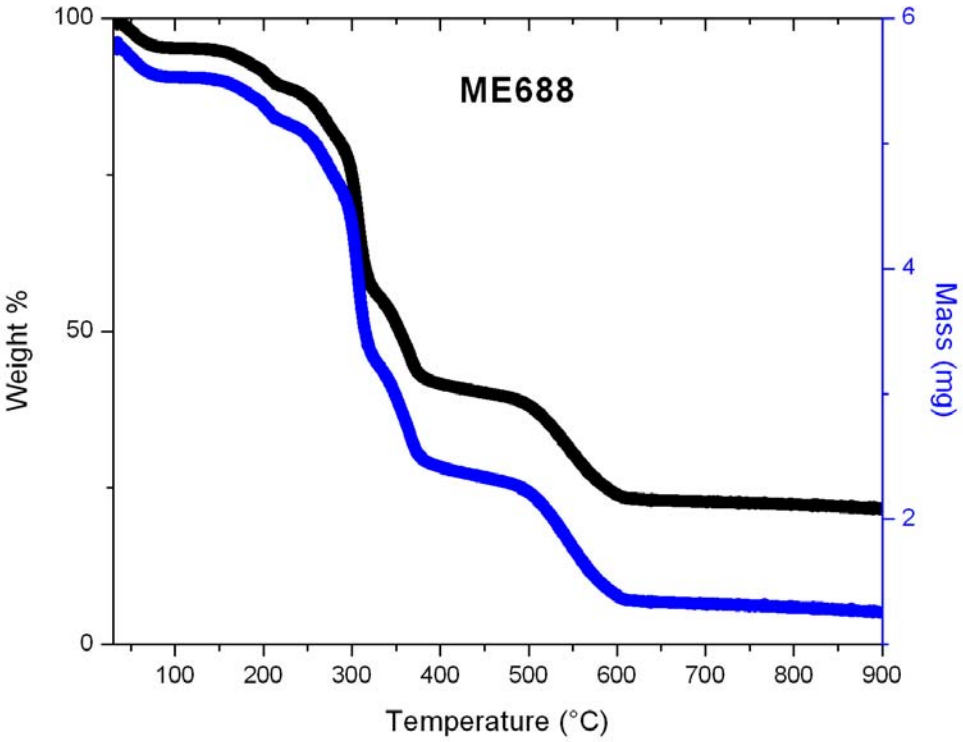

**Appendix III: UV-Visible Spectroscopy**

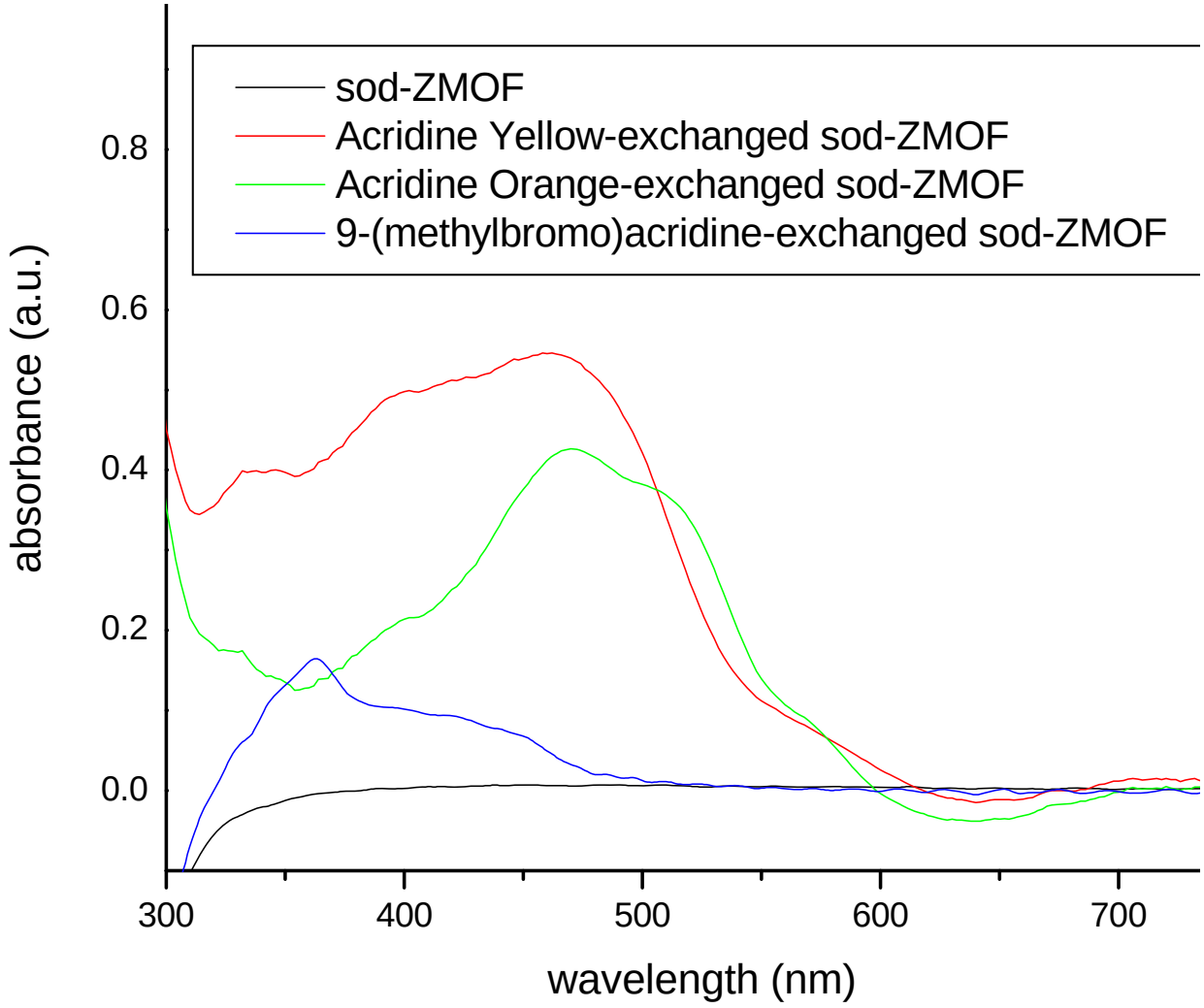

**Appendix III (continued)**